

Nano-biomechanical investigation of living endothelial cells

Ph.D. Thesis

Attila-Gergely Vég

Supervisor: Dr. György Váró

Institute of Biophysics, Biological Research Centre
Hungarian Academy of Sciences

Szeged

2012

Table of Contents

List of publications.....	iii
Abbreviations.....	v
1 Introduction.....	1
1.1 Biomechanics	1
1.2 Single cell micromanipulation.....	2
1.3 Scanning the micro world.....	3
1.3.1 Atomic force microscope.....	3
1.3.2 High-resolution imaging	4
1.3.3 Mechanotesting.....	5
1.4 Cellular biomechanics	7
1.4.1 Role of cytoskeletal components	7
1.4.2 Role of plasma membrane	8
1.4.3 Cell mechanics related pathologies.....	9
1.5 Insight into mechanobiology of the BBB	10
1.5.1 Cerebral endothelial cells.....	10
1.5.2 Cellular extravasation – diapedesis.....	11
1.6 The aim of the study.....	12
2 Matherials and Methods.....	13
2.1 Cell Culture	13
2.2 Instrumentation.....	13
2.3 Single force spectroscopy.....	14
2.3.1 Hertz model	15
2.3.2 Force Volume Mapping.....	16

2.3.3	Adhesion decomposition.....	16
2.3.4	Relaxation parameters.....	16
3	Results	18
3.1	Morphology of cerebral endothelial cells.....	18
3.2	Elasticity of cerebral endothelial cells.....	20
3.2.1	Spatial elasticity.....	21
3.2.2	Temporal elasticity	22
3.3	Intercellular mechanics.....	24
3.3.1	Adhesion	26
3.3.2	Stress relaxation.....	28
4	Discussion.....	30
4.1	Heterogeneities in spatio-temporal elasticity of cerebral endothelial cells	30
4.2	Insights into intercellular mechanics of endothelial cell layer tested with melanoma cell as a probe	32
5	Summary.....	35
6	References.....	37
	Acknowledgement	48
	Annex	49

List of Publications

Full papers directly related to the subject of the thesis

- I. **Végh, A. G.**; Fazakas, C.; Nagy, K.; Wilhelm, I.; Molnár, J.; Krizbai, I. A.; Szegletes, Z.; Váró, G. Adhesion and Stress Relaxation Forces between Melanoma and Cerebral Endothelial Cells. *Eur. Biophys. J.* **2012**, *41*, 139-145.
IF: **2,286** Times Cited: **0** Independent citations: **0**
- II. **Végh, A. G.**; Fazakas, C.; Nagy, K.; Wilhelm, I.; Krizbai, I. A.; Nagyősz, P.; Szegletes, Z.; Váró, G. Spatial and Temporal Dependence of the Cerebral Endothelial Cells Elasticity. *J. Mol. Recognit.* **2011**, *24*, 422-428.
IF: **2,387** Times Cited: **0** Independent citations: **0**

Full papers directly not related to the subject of the thesis

- III. **Végh, A. G.**; Nagy, K.; Bálint, Z.; Kerényi, A.; Rákhely, G.; Váró, G.; Szegletes, Z. Effect of Antimicrobial Peptide-Amide: Indolicidin on Biological Membranes. *J. Biomed. Biotechnol.* **2011**, *2011*, 670589.
IF: **1,225** Times Cited: **0** Independent citations: **0**
- IV. Miclea, P. S.; Péter, M.; **Végh, G.**; Cinege, G.; Kiss, E.; Váró, G.; Horváth, I.; Dusha, I. Atypical Transcriptional Regulation and Role of a New Toxin-Antitoxin-Like Module and its Effect on the Lipid Composition of *Bradyrhizobium Japonicum*. *Mol. Plant Microbe Interact.* **2010**, *23*, 638-650.
IF: **4,010** Times Cited: **1** Independent citations: **0**
- V. Bálint, Z.; Nagy, K.; Laczkó, I.; Bottka, S.; **Végh, G. A.**; Szegletes, Z.; Váró, G. Adsorption and Self-Assembly of Oligodeoxynucleotides Onto a Mica Surface. *Journal of Physical Chemistry C* **2007**, *111*, 17032-17037.
IF: **3,333** Times Cited: **5** Independent citations: **4**

- VI. Bálint, Z.; **Végh, A. G.**; Popescu, A.; Dima, M.; Ganea, C.; Váró, G. Direct Observation of Protein Motion during the Photochemical Reaction Cycle of Bacteriorhodopsin. *Langmuir* **2007**, *23*, 7225-7228.
IF: **4,009** Times Cited: **5** Independent citations: **5**
- VII. Wilhelm, I.; Farkas, E. A.; Nagyószzi, P.; Váró, G.; **Végh, A. G.**; Couraud, P.; Bálint, Z.; Weksler, B.; Krizbai, I. A.; Romero, A. I. Regulation of Cerebral Endothelial Cell Morphology by Extracellular Calcium. *Physics in Medicine and Biology* **2007**, *52*, 6261-6274.
IF: **2,528** Times Cited: **9** Independent citations: **3**
- VIII. Vollmer, J.; **Végh, A. G.**; Lange, C.; Eckhardt, B. Vortex Formation by Active Agents as a Model for Daphnia Swarming. *Phys. Rev. E. Stat. Nonlin Soft Matter Phys.* **2006**, *73*, 061924.
IF: **2,438** Times Cited: **8** Independent citations: **8**

Scientometric data:

- Total number of published articles: **8**;
- Total impact factor: **22,216**;
- Total citations: **28** Independent citations: **20**.
- Hirsch-Index: **4**

Abbreviations

AC	– A lternate C ontact
AFM	– A tomic F orce M icroscopy
BBB	– B lood- B rain B arrier
CAM	– C ell A dhesion M olecule
CEC	- C erebral E ndothelial C ells
CHO	- C hinese H amster O vary
CNS	– C entral N ervous S ystem
ConA	– C oncanavalin A
EBM	– E ndothelial B asal M edium
EGM	– E ndothelial G rowth M edium
FBS	– F etal B ovine S erum
FV	– F orce V olume
FVM	– F orce V olume M apping
hCMEC/D3	– h uman C erebral M icrovascular E ndothelial C ells / D3
HUVEC	– H uman U mbilical V ein E ndothelial C ells
LAD	– L eukocyte A dhesion D eficiency
MFP-3D	– M olecular F orce P robe – 3D
PBS	– P hosphate- B uffered S aline
RPMI	– R oswell P ark M emorial I nstitute
SCFS	– S ingle- C ell F orce S pectroscopy
SPM	– S canning P robe M icroscopy
YM	– Y oung’s M odulus

1 Introduction

1.1 Biomechanics

By applying rules of classical mechanics for studying structure and function of living organisms, the still enlarging field of biomechanics emerges. Ranging from multi- to single-cellular organisms and even down to sub cellular processes, it has an amazing power of description, approximation and prediction. Knowledge development in biomechanics offers deeper insights into physiological functions and provides improved treatment for a constantly widening range of pathologies.

The first steps of biomechanics date back to the Middle Ages, most probably to those times, when Leonardo da Vinci tried to improve the yield of horse power by mechanical approach. However, the book, which can be regarded as the first study on biomechanics, dates back to the second half of the seventeenth century by Giovanni A. Borelli. In his work, entitled *De Motu Animalium I-II*, comparison is made between animals and machines with help of mathematics to prove the theories. Even though, modern science treats biomechanics as a self-standing field. It was only in the late sixties, when the emergence of new technologies and the need for a predictive science, facing biology related questions triggered its renaissance. As biomechanics and engineering are strongly connected, analysis of biological systems is often based on traditional engineering methods.

As scientific research has been turning towards microscopic sizes, the field of biomechanics has been extending too. Knowledge on surgical implant design, development of joint replacement (Bozic et al. 2012; Jazayeri and Kwon 2011), blood flow modeling (Anor et al. 2010), skeletal muscle and bone mechanics (Burr 2011), tissue stress resistance, cell motility (Levayer and Lecuit 2012), intercellular adhesion (Trepap and Fredberg 2011) have evolved enormously over the last few decades. Noteworthy scientific research efforts have been focused to discover and describe links between human diseases and biomechanics. Simple applications of Newtonian mechanics and/or materials sciences often provide good approximations to the mechanics of many biological systems. With the constantly enlarging knowledge accumulated from these

areas, research and technology provides deeper and deeper insight towards nano-, or even picometric scale.

Mechanics plays a crucial role in many cellular processes. Influence of cellular, sub-cellular and molecular mechanics on human disease states, including cancer (Suresh 2007), has gained quickly expanding scientific interest recently. Several questions were addressed and answered in this area, concerning cell ultrastructure, cellular and cytoskeletal mechanical properties, elastic deformation characteristics etc.

Research of biomechanics not only reveals the mechanics related origins of many diseases, connects the physiology and function, but can improve the treatment of many pathological events as well.

1.2 Single cell micromanipulation

Despite the richness offered by modern imaging techniques, only a fraction of them furnishes data on living tissue or cell. Moreover, interest on single cell dynamics led to development of powerful micromanipulation technologies.

Cell must suffer a certain deformation upon a known force, which deformation is needed to be measured. Several different techniques have been introduced for single cell handling and testing. Micropipette aspiration extends the cell's surface by partially aspirating it (Hochmuth 2000). Optical tweezers trap the cell or test it with a trapped microbead (van Mameren et al. 2011). Magnetic twisting cytometry uses 1-10 micrometer size ferromagnetic microbeads to apply shear stress on the cell's membrane (Wang et al. 1993). Atomic Force Microscope (AFM) indents the cell surface with constant velocity using an arbitrary shape indenter.

This list is far not complete, where each has its own strength and weakness. AFM has a considerable advantage over the aforementioned instruments. It provides three dimensional topography and ability of mechanical testing simultaneously. Operating in liquid over large range of temperatures, make it spread quickly in life sciences. Its detailed description is the subject of the next section.

1.3 Scanning the micro world

As a branch of micromanipulation development, which later has quickly spread in life sciences, a large range (from micro to pico scale) imaging instrument family emerged: the Scanning Probe Microscope (SPM) superfamily. The inherited name of microscope is somewhat misleading since they have not too much in common with conventional microscopes. However, if we look at the high-resolution images they provide, they indeed deserve the term ‘microscope’. The vast areas of interest have led to numerous instrument types to be developed. Fortunately for science, the family is so large, that their complete physical and methodical description, or even enumeration would be a challenging task, and that points far beyond the aim of this study. It should be noted that not all of them exert or detect direct mechanical forces on the studied specimens.

Bringing to life the concept of “touching” individual atoms, the key feature of every member of this large family is the very sharp tip on a cantilever used as a probe. They are so sharp, their apex consist of only a few atoms. Consequently, direct inter-atomic forces can be measured with high accuracy. Depending on the requirements of the field in which they are applied, the cantilever and the tip are usually made of a large variety of materials: tungsten, platinum/iridium, silicon nitride, carbon or gold, just to name a few. Tip shape and cantilever stiffness can be chosen accordingly to experimental setup; from ultra sharp to micron sized colloidal probes, from extra soft to high rigidity and conductivity cantilevers.

1.3.1 Atomic force microscope

Probably the most relevant member of the instrument family for biological investigations at micro-scale is the Atomic Force Microscope. It was invented in the early eighties by Gerd Binnig and his co-workers (Binnig et al. 1986). At that time Binnig and Heinrich Rohrer, was awarded with Nobel prize “for their design of the scanning tunneling microscope”, which was the precursor of the AFM.

Briefly, the AFM monitors the forces at the level of and between single atoms, which explains the term ‘atomic’. To achieve this, a very sharp ‘needle’ is brought into contact with the sample to be investigated. At the theoretical edge, a single atom of the tip interacts with a few (or single) atoms of the sample. Although this requires special

circumstances and sample preparation, the ranges of measured forces are at the level of piconewtons, or even below.

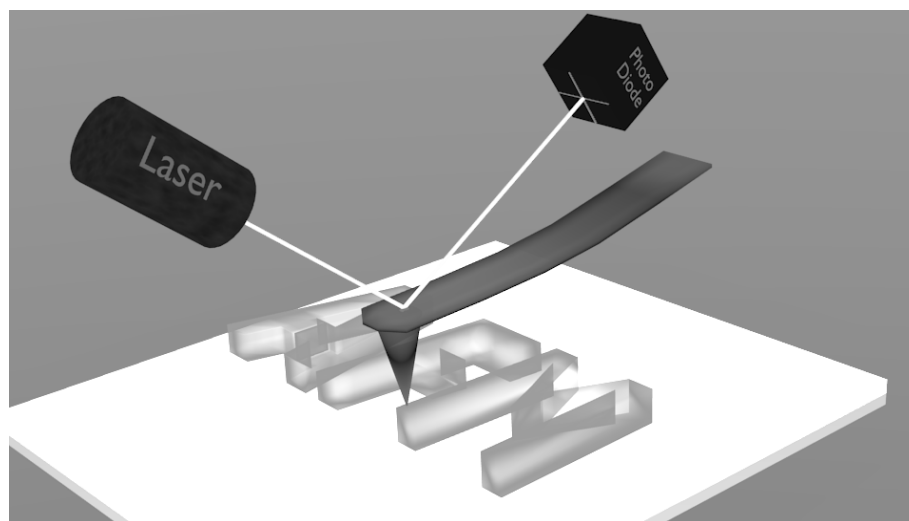


Figure 1. Schematic view of AFM

High-resolution images require high accuracy actuators to move the tip along the surface of the sample, and record its interactions line by line, point by point. The high resolution is provided by an accurate detection system, based on piezo controlled motion and laser positioning. As Figure 1 depicts, the tip is positioned at the end of a soft and a relatively long cantilever, a narrow laser beam is reflected from its top, which is detected by a four-segment photodiode. Vertically, it provides sub-nanometer resolution, while horizontally the tip-sample convolution is needed to be taken into consideration at final analysis.

Atomic Force Microscope is a rather old member of the SPM superfamily. Its technology offers powerful ways for *in vitro* biological applications concerning cellular mechanics and morphology. As it can operate in liquid environment and at human body temperature, it became the most reliable and accurate nanoforce-tool in the research of cellular biomechanics. Nevertheless, the ability of nanometer scale mechanical manipulation and measurement in a liquid environment on living cells is an absolute advantage compared to conventional cellular imaging techniques.

1.3.2 High-resolution imaging

Non-invasive, sub-nanometer resolution imaging in liquid at human body temperature, puts the AFM at the leading front of biophysical investigations of

biomaterials. It is suitable for applications at large scale range, from living cells (Bálint et al. 2007a) through membranes (Végh et al. 2011) down to single molecules (Bálint et al. 2007b; Gad et al. 1997; Karsai et al. 2006), covering over four orders of magnitude.

Basically two different imaging modes can be distinguished: “Contact” and “Alternate Contact” (AC) or tapping mode. During raster scan, in “Contact mode”, the deflection of the cantilever is kept constant by a feedback loop. In “AC mode”, the cantilever oscillates at its resonant frequency and the feedback loop minimizes the amplitude deviations. As three-dimensional topography is recorded during scans, no posterior data processing is required to reconstruct three dimensional images.

Acquisition of one image, depending on resolution and scanning rate applied, is at the order of minutes. However, even video rate AFM is available on the market (Ando et al. 2008; Picco et al. 2007), but due to its special sample preparation and limited scan size it is less used in life sciences. On the other hand, combination with other techniques provides considerable improvements of simultaneous investigations (Deckert-Gaudig and Deckert 2011; Kellermayer 2011).

1.3.3 Mechanotesting

Beside non invasive and high resolution imaging, it provides valuable data as a nanomechanical tester, even simultaneously in many cases. Starting from single molecule spectroscopy, through membrane dynamics up to cellular level studies, it represents an invaluable tool for *in vitro* micromanipulation experiments.

Among its many interesting features, such as direct measurement of protein conformational change (Bálint et al. 2007c), friction measurement (Coles et al. 2008), microlithography (Davis et al. 2003) etc., acquisition of force-distance curves, is outstanding. As an accurate micromechanical tester, offers wide range of possibilities in living cell biomechanics (Bálint et al. 2007a; Carl and Schillers 2008; Franz and Puech 2008).

Force curves can be achieved simply by lowering (trace) the probe onto the sample, until a pre defined bending of the cantilever is reached, and pulling back (retrace) to initial position. The basic force curve holds the deflection vs. the vertically travelled distance of the cantilever (Figure 2, panel a). Based on these curves, many useful parameters can be calculated, but their holistic enumeration points beyond the limits of this study. Only the most relevant ones, used in our experiments, are discussed hereby.

The most widespread and employed parameter as a measure of stiffness is the tensile or elastic modulus. Based on Hooke's theorem, this parameter quantifies the ability of a given material to withstand stress. By recording a usual load-distance curve, the sample's Young's Modulus (YM) can be calculated (Vinckier and Semenza 1998). On the panel a of Figure 2, zero distance marks the probe-sample contact. As a reference, the cantilever's own deflection needs to be eliminated, simply by subtracting a force curve recorded on hard surface, e.g. Petri dish. The obtained force-indentation curve between contact point and maximal trigger point, gives the sample's YM.

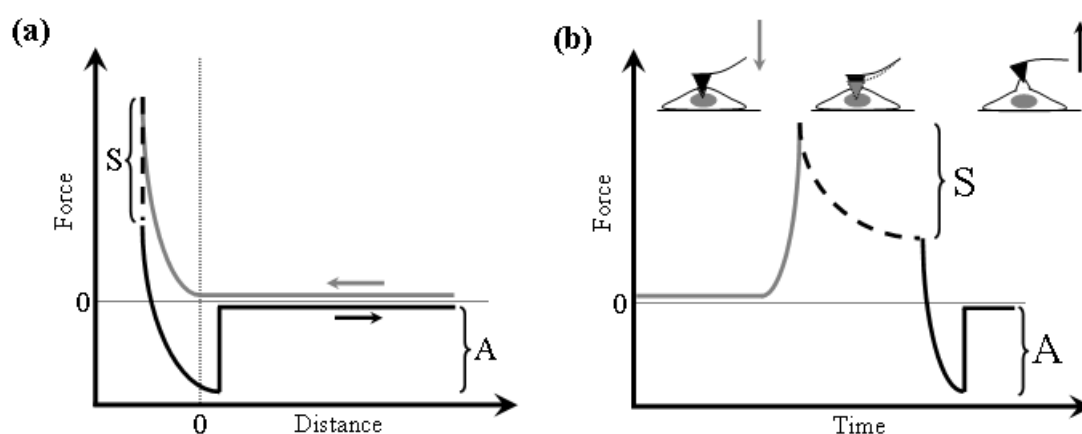


Figure 2. Schematic force curve of soft material. (a): force vs. distance. (b): force vs. time. Trace is plotted with light grey, points in dwell time are dashed and retrace is shown in black. A = adhesion force; S = Stress relaxation force.

Another important parameter is the adhesion, denoted with A on Figure 2. Regardless of its origin, real time probe-sample adhesion can be monitored with high accuracy (Benoit and Selhuber-Unkel 2011). As biochemical and biophysical signaling of living cells relies on protein-protein interactions, protein functionalized probe – cell surface adhesion is an *in vitro* technique to test receptor-binding forces with AFM. It consists of applying a constant and controlled force to a receptor-ligand bond. As a result, dissociation lifetime can be measured (Robert et al. 2008; Wojcikiewicz et al. 2006; Yuan et al. 2000).

In reality, none of the materials behaves purely as Hooke's law predicts. Both viscous-like and elastic characteristic are present upon mechanical strain. The manner how a material relieves stress under constant strain is described by stress relaxation. AFM is a good candidate to detect relaxation of various materials, e.g. living cells. On Figure 2, stress relaxation is marked with S, and it is depicted by the small pictogram in the middle

of the b panel. Beyond a certain recording speed, relaxation emerges what can be visualized by plotting the force-distance curves against time (Figure 2, panel b). At recording speed comparable with reorganization velocity, relaxation is hindered.

1.4 Cellular biomechanics

From the dynamic pushing & pulling during tissue development, cells in their native environment are subjected to constant processing of mechanical signals, implying continuous control on morphology and adhesion. Cellular morphology is strongly related to survival and reproduction ability too, therefore any alteration might be fatal; outer structure and adhesive properties are strongly interconnected (Iyer et al. 2009). Consequently, cell motility is determined by connections between cytoskeleton and intercellular junctions as well as by interacting molecules to the extracellular matrix. Multicellular organisms rely on proper adhesion between individual cells and interconnecting tissue. Binding to a surface or to another cell may be crucial even for unicellular organisms (Ubbink and Schar-Zammaretti 2005; Zhang et al. 2011).

Structure and cellular micro- or nanomechanical properties are strongly interconnected. Their understanding is essential to improve treatment of pathologies. Stiffness alterations of blood-travelling cells might have pathologic consequences; however, it is difficult to measure their elasticity, due to their mobile nature. Nevertheless, interesting ways for immobilization and measurements were introduced in their research (Dulinska et al. 2006).

Elastic properties of surface adherent cells are mostly determined by cytoskeletal and membrane components (Kumar and LeDuc 2009). Cytoskeletal polymer organization and membrane fluidity are the most important components, which determine cell morphology and elasticity.

1.4.1 Role of cytoskeletal components

The ability of eukaryotic cells to support deformation, to exert forces, to move intracellular load relies on the cytoskeleton, which is an interconnected network of polymer filaments and auxiliary proteins. Three main polymer types can be distinguished: actin filaments, microtubules and intermediate filaments. All network components differ

in polarity, assembly dynamics, stiffness and the molecular motors they associate with (Fletcher and Mullins 2010).

Assembly dynamics consists of a constant equilibrium between polymerization and depolymerization of network components. Apparent elasticity is influenced by internal heterogeneities too. Intermediate filaments and microtubules form a dense network all over the cell, the latter being organized by microtubule-organizing centers. Actin filaments densely interconnect the cytoplasm close to membrane's inner surface. Mechanical properties of cell cortex differ remarkably from deeper parts. For small indentation depths, the network of actin filaments dominates over other components regardless of cell type (Pogoda et al. 2012).

By comparing the resulted strain upon stress of the individual polymer types, microtubules were found to be more rigid, followed by intermediate and the actin filaments (Janmey et al. 1991). Blocking actin polymerization induces decrease in relative elastic modulus of epithelial cells. Beside this, elasticity alterations can be caused by the collective action of myosin motor proteins (Schillers et al. 2010). Oppositely, blocking microtubule disassembly induces cell stiffening (Kim et al. 2012). As all cytoskeletal networks are in continuous and dynamic reorganization, cell stiffness is highly determined by their orchestrated cooperation. For few hundred nanometer deep penetrations, dominance of actin filaments in apparent cellular elasticity is accepted.

1.4.2 Role of plasma membrane

Cell membrane or plasma membrane, plays a central role in cell mechanics. Among many important functions, it constitutes the interface between inner and outer compartments and incorporates anchor points for cytoskeletal network components, which determines the shape of the cell. Besides, it holds the outer glycocalyx, which contributes to the apparent cell stiffness too (O'Callaghan et al. 2011). Direct effect of membrane fluidity on apparent cell stiffness is an interesting question. Selective membrane crosslinking resulted two fold increase of cell elasticity (Wu et al. 1998).

Plasma membrane incorporates the cell adhesion molecules which might be distributed randomly or may form distinct clusters. Generally intercellular adhesion is initiated by cell-adhesion molecules (CAM) (McNamee et al. 2007), interacting with their extracellular ligands, similar to the lock-and-key principle. These proteins can be divided into four families: the immunoglobulin-like adhesion molecules, integrins, cadherins and

selectins (Buckley et al. 1998). Except the first, all are calcium dependent, hence extracellular calcium plays key role in cell-cell adhesion (Wilhelm et al. 2007).

Cell-adhesion requires alignment of several weak bonds to yield specificity. The relative weakness of these bonds offers many possibilities to cells to easily manipulate the strength of their adhesion.

1.4.3 Cell mechanics related pathologies

Many of the leading diseases of global mortality are related more or less to cell mechanics. Viral and microbial binding to host cells or tissues (Liu et al. 2010) and metastasizing cells (McNamee et al. 2007) are typical examples. Effect of man derived air pollution on human health is under constant debate with constantly enlarging interest (Wu et al. 2012). Red blood cells need to sustain their plasticity when passing through micro capillaries. Decreased deformability of malaria (*Plasmodium falciparum*) –infected erythrocytes affects their ability to pass through micro channels (Shelby et al. 2003). Immature blood cells show uncontrolled proliferation in acute leukemia. Increased adhesion and decreased deformability are thought to be connected to their accumulation in vasculature (Lichtman et al. 1973). Lymphocytes of diabetic mice were found to be stiffer than control ones (Perrault et al. 2004). Leukocyte mobilization, migration and adhesion is crucial in immune surveillance against pathogens. Defects of adhesion molecules involved in this complex process, lead to Leukocyte Adhesion Deficiency (LAD) (Hanna and Etzioni 2012).

Metastasizing cells alter their shape and adhesion in order to be able to travel along the organism to form new colonies far from primary tumors. It has been previously proven that cancerous cells show considerable differences, compared to non-cancerous ones (Li et al. 2008). Their biomechanical properties undergo certain change in order to sustain non controlled development and survival (Kumar and Weaver 2009). While the division rate of these cells is higher, their biomechanical properties need to go through dramatic adjustments. Deeper insight into mechanical properties offers better understanding of morphology and adhesion related processes.

Even though, differences between several cell types or interaction with well defined surfaces can provide interesting results. Describing differences of normal and malign cells (Cross et al. 2007) leads to better knowledge of their metastatic potential. Many studies have reported coherently that malignant cells show lower stiffness and

higher elastic properties (Rosenbluth et al. 2006; Docheva et al. 2008). Beside this, their morphology involves structural changes, which goes hand in hand with elastic properties.

1.5 Insight into mechanobiology of the BBB

1.5.1 Cerebral endothelial cells

Endothelial cells have a distinguished role in many mammalian organisms. As they cover the inner vessel walls, they have distinct and unique functions in vascular biology. Fluid filtration, blood vessel tone, hemostasis, hormone trafficking, neutrophil recruitment are only a few items on their task-list.

Among endothelial cells, the cerebral endothelial cells (CECs) have probably the most prominent role: they form the morphological basis of the blood-brain barrier (BBB). This is an active, double sense interface, having barrier function for toxins and at the same time a carrier function for nutrients and metabolites to and from the Central Nervous System (CNS). Therefore, the BBB has an outstanding importance concerning many known pathologies related to the CNS. Meningitis, human immunodeficiency virus encephalitis, Alzheimer's disease, rabies, multiple sclerosis, epilepsy, metastasizing tumors, ischemia just to name a few in which the BBB is more or less involved (Rosenberg 2012).

The CECs provide such a tight barrier, that both the paracellular and transcellular traffic of molecules and cells is highly regulated and coordinated. At their intercellular junctions, many adhesion and channel forming molecules help to maintain the proper physiology and function. However, it is highly permeable for small lipid soluble molecules, among which caffeine and alcohol are the most exploited by markets. Despite these small gaps for lipid-soluble molecules, drug delivery to the CNS is considerably limited.

CECs are very sensitive to environmental changes (Wilhelm et al. 2008; Wilhelm et al. 2007), therefore in some pathological cases their mechanical modulation can reversibly open the BBB (Bálint et al. 2007a). Circulating factors within the blood can alter their mechanical properties (Lee et al. 2011). Inorganic salts (Oberleithner et al. 2009; Oberleithner et al. 2007) and nitric oxide (Fels et al. 2010) are well-studied regulators of endothelial elasticity.

Endothelial cells have a prominent role in wound healing (van der Meer et al. 2010) and angiogenesis too, which relies on rapid changing and adaptability of their mechanical parameters. Many internal stimuli and external mechanical stress affects endothelial migration. Shear stress enhances wound closure *in vitro*, by modulating cell migration velocity and increasing apparent cell area (Albuquerque et al. 2000).

Biomechanical investigation of endothelial cells is a very important and growing field in science. Unfortunately, the range of available literature for different cell types is somewhat limited, moreover, relatively little knowledge is gathered about CEC's mechanical properties. Morphology and spatio-temporal elasticity of different endothelial cultures will be presented: sub-confluent living, confluent living and confluent but paraformaldehyde fixed cell cultures will be compared.

1.5.2 Cellular extravasation – diapedesis

In case of inflammatory processes, the immune system activates the leukocytes, which can cross the blood vessels in order to fight infections or intrusive pathogens. Cellular extravasation is a complicated process involving many steps, as described in case of leukocytes (Greenwood et al. 2011).

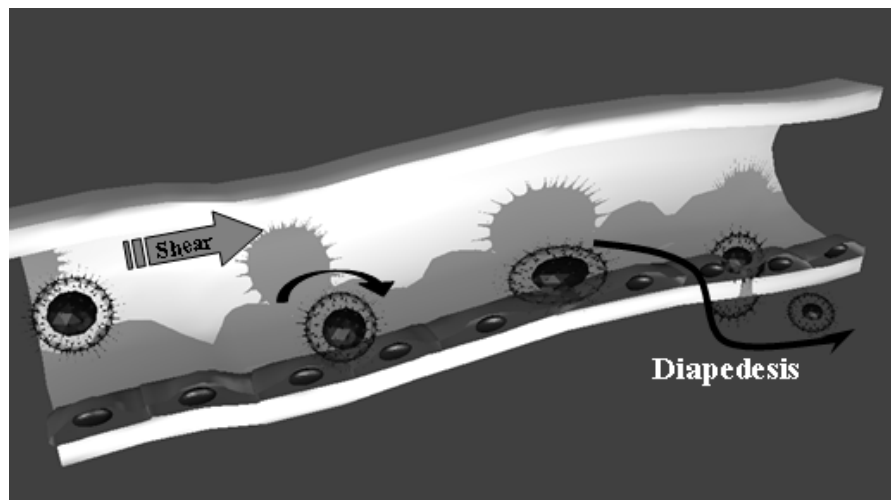


Figure 3. Schematic view of plausible melanoma-endothelial transmigration process

Primordially to cross the endothelial layer, the first step is the rolling/capture of leukocyte, succeeded by chemokine activation and firm adhesion/arrest. After this, crawling and diapedesis occurs. Extravasation requires the successive formation and breakage of cell-cell contacts between leukocytes and endothelial cells lining the vessels

(Muller 2011). A class of cell-adhesion molecules that are specific for leukocyte – vascular cell interactions, mediates these contacts.

For metastasizing tumor cells that spread through the circulatory system, the use cell adhesion-related mechanisms are thought to be primordial to establish new tumors in the body, however, details of this process are under debate. As the brain lacks a lymphatic system, role of the BBB for metastasizing cancerous cells to enter the CNS is crucial. Figure 3 depicts plausible similarities to leukocyte-endothelial transmigration, although the exact details of this process are not exactly known. *In vitro* cell co-culture models dealing with the whole process have already been successfully established (Wilhelm et al. 2011). Static models involving co-culturing do not provide data on adhesion dynamics or strength.

Anti-metastatic drugs may have selective affinity upon targeting only adhesion related step of the whole process. Specific adhesion between living melanoma cell and a colloid particle has already been measured successfully by AFM. Surface charge and hydrophobicity appeared to alter cell-particle adhesion (McNamee et al. 2006). This is a good method to test specific drugs acting on different CAMs.

In this study, we present intercellular adhesion measured at physiological conditions between living melanoma and living endothelial layer. Adhesion strength dependence upon load and dwell time is presented. Furthermore, adhesion force decomposition and parameters of total stress relaxation are determined.

1.6 The aim of the study

- To describe and compare the morphology and the spatio-temporal elasticity of sub-confluent and confluent living CECs
- To characterize the changes in morphology and elasticity induced by paraformaldehyde fixation on living endothelial cell layer.
- To establish cell-cell adhesion experiments on living cells and to quantify the intercellular adhesion between living melanoma and cerebral endothelial monolayer
- To monitor total stress relaxation force of melanoma cells brought into contact with living and fixed CEC monolayer

2 Materials and Methods

2.1 Cell Culture

Human cerebral endothelial cells (hCMEC/D3 - shortly D3) were grown on rat tail collagen-coated dishes in EBM-2 medium (Lonza) supplemented with EGM-2 Bullet Kit (Lonza) and 2.5% FBS from Sigma (Wilhelm et al. 2008; Wilhelm et al. 2007). B16/F10 melanoma cells were kept in RPMI medium (Sigma) supplemented with Glutamax and 5% of Fetal Bovine Serum (FBS) from Lonza. Cultures used as sub-confluent, were measured shortly after passage, as soon as all cells adhered to Petri dish.

All measurements were carried out in Leibovitz medium (Sigma) at 37°C within 3 hours after taking the cells out from the incubator. According to our observations, within this period cells preserve their viability. Leibovitz medium was chosen due to its pH stabilization ability, hence circumventing usage of ambient CO₂.

Cell fixation was performed using 4% paraformaldehyde solution for 30 minutes, followed by buffer rinsing with PBS (2.7 mM KCl, 1.5 mM KH₂PO₄, 0.136 M NaCl, 0.5 mM Na₂HPO₄), prior to experiments. During fixation the Petri dish with cell layer was not removed from the microscope stage.

2.2 Instrumentation

All measurements were performed with an Asylum Molecular Force Probe - 3D (MFP-3D) head and controller (Asylum Research), using MFP-3D Xop driver program written in Igor Pro software (version 6.22A, Wavemetrics). For single cell elasticity measurements, gold-coated silicone nitride rectangular cantilevers with “V” shaped tips (Olympus, Optical Co. Ltd.), while for cell-cell adhesion measurements aluminium backside coated tipless cantilevers were used (MikroMasch). Their spring constant was determined by thermal calibration (Hutter and Benchoefer 1993), resulting in 0.03 N/m in both cases, while their resonant frequency in liquid was 7 and 10 kHz respectively.

Images were recorded typically in Alternate Contact (AC) mode having 256 lines by 256 points, at a tip velocity of 60 $\mu\text{m/s}$. By comparing trace and retrace, noteworthy differences were not observed, which underlines the reliability of the images.

Living cells were scanned in their own Petri dish, in Leibovitz medium. As their adhesion to the collagen-coated surface is firm enough, there was no need for extra immobilization method.

2.3 Single force spectroscopy

All force curves were recorded at constant loading rate and sampling frequency. In case of single force measurements for spatio-temporal elasticity a load rate of 0.6 $\mu\text{m/s}$, for elastic maps 6 $\mu\text{m/s}$, while for intercellular adhesion curves 2 $\mu\text{m/s}$ was applied. Data was collected at a sampling frequency of 2 kHz and a maximum load below 1 nN was used. Total force distance was set to 3 μm for single elastic curves, 2.5 μm for FVM, and 8 μm for cell-cell measurements. In case of intercellular measurements the applied load varied from 0.5 nN up to 5 nN. Dwell time ranged from 0 up to 30 seconds.

Ten forces were recorded for each load (respectively dwell time) starting from low up to high values successively, followed by reverse direction recording from high to low values. Finally, the averages and standard deviations of corresponding values were calculated, and presented. Using this technique we eliminated the possible tip-induced alterations of applying unidirectional variation of load and dwell time.

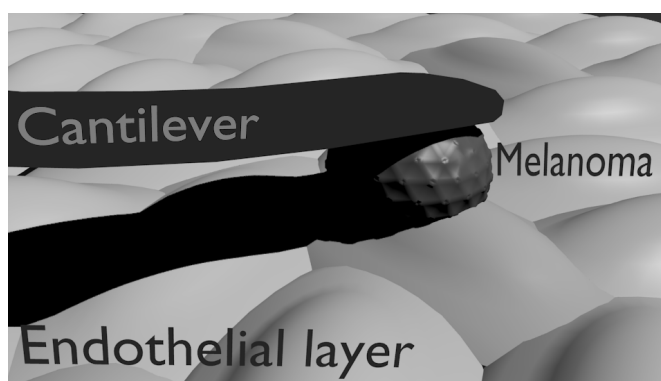


Figure 4. Schematic representation of intercellular measurement.

Figure 4 depicts schematic view of intercellular measurement with single cell probe, used in our experiments. The individual melanoma cells were attached to the

tipless cantilever using a Concanavalin-A (Con A) – mediated linkage (Zhang et al. 2006). With the help of an Axiovert 200 microscope, the cantilever was lowered gently onto a melanoma cell, for approximately one second to attach the cell to its end. This step was followed by bringing the “cell probe” and the monitored surface into contact. After each set of measurement, the melanoma’s position has been checked. No considerable changes were observed.

2.3.1 Hertz model

Probing any material with an AFM tip, leads to the theory of indenting an elastic half-space with a stiff object. Based on work of Heinrich Hertz (Hertz 1882) and Ian Sneddon (Sneddon 1965), later modified for AFM tips (Mathur et al. 2001), this theory is widely used for indentation tests, regardless of length scale.

At each measurement, the deflection of the cantilever and the indentation of the sample is recorded simultaneously. The latter can be obtained by subtracting the bare cantilever’s deflection values recorded on a hard surface. The force as a function of the indentation Δz , considering a conical tip with opening angle α is described by the equation:

$$F(\Delta z) = \frac{2E^*}{\pi(\tan(\alpha))} \Delta z^2 \quad (1)$$

where E^* , the relative Young’s modulus is:

$$\frac{1}{E^*} = \frac{1 - \mu_{cantilever}^2}{E_{cantilever}} + \frac{1 - \mu_{sample}^2}{E_{sample}} \quad (2)$$

Considering that the cantilever is made of silicon or silicon nitride, which is several orders of magnitudes harder than the sample ($E_{sample} \ll E_{cantilever}$) the above equation can be simplified:

$$\frac{1}{E^*} \approx \frac{1 - \mu_{sample}^2}{E_{sample}} \quad (3)$$

In this case E_{sample} is the Young’s Modulus and μ_{sample} is the Poisson ratio of the cell (Vinckier and Semenza 1998). In eq. 1, the exponent of Δz varies according to the indenter’s geometry. It takes the value of 2 for a sharp conical tip, 1.5 for a sphere and 1 for punch shaped indenter. For a review see (Azeloglu and Costa 2011).

2.3.2 Force Volume Mapping

Elasticity map of living endothelial cells was recorded by performing Force Volume Mapping (FVM). Prior to FVM, an image on the area of interest was recorded and divided into 32 lines by 32 points. At each point, a force curve with total distance of 3 μm was effectuated at a loading rate of 6 $\mu\text{m/s}$. Lateral tip velocity was set to 60 $\mu\text{m/s}$.

A color coded elasticity map was calculated by taking the Young's Modulus, described in previous section (eq. 1-3), as the elastic parameter. Simultaneously adhesion map was calculated, based on total unbinding forces of retrace curves. As an internal reference, height map was reconstructed based on calculated contact point of each curve. Compared to prior recorded image, no considerable differences can be found.

2.3.3 Adhesion decomposition

A homemade MatLab (MathWorks) routine has been developed to extract the total adhesion force values, statistics of force ruptures and stress relaxation amplitudes. If not stated otherwise, the total adhesion force was defined as the total unbinding strength. It was quantified as the level difference between the maximal downward deflection point of the cantilever and the average of last ten points.

Individual jumps on retract curves were identified as the level difference between two adjacent points passing a threshold. Two fold of the standard deviation taken from the last 50 points of each curve was given as threshold. Using the above-mentioned routine, number and size of individual jumps were detected for each force curve. For each parameter set, twenty forces were taken in previously described manner (see. Page 14 for details), and the Average \pm Standard Deviation values were plotted at each graph.

For comparison of live and fixed endothelial layer, rupture values detected on all curves of the respective set, were used.

2.3.4 Relaxation parameters

Stress-relaxation response upon a defined sudden displacement is widespread method to determine the viscoelastic parameters of a material. The solution for a hard spherical indenter testing an isotropic, incompressible material appropriately describes

majority of experimental data (Darling et al. 2006; Moreno-Flores et al. 2010a). Unfortunately only qualitative description can be applied, as a cell layer tested by a second cell does not fulfill the previously mentioned requirements.

Total stress relaxation amplitude was calculated as the difference between maximal upward deflection force and its value at end of dwell time. On Figure 2 this is denoted with S . A biexponential decay (eq. 4) described our data in good quality.

$$S(t) = \alpha + A_f e^{\frac{-t}{\tau_f}} + A_s e^{\frac{-t}{\tau_s}} \quad (4)$$

α accounts for a purely elastic response, while indices “f” denote the fast decaying component, while s the slow decaying component. These parameters are plotted on Figure 17, calculated at different dwell times on several loads. Each decaying element acts as an individual relaxation process and their total sum provides the overall response. Presumptively we can assign each cell with one element, but a rigorous description requires further experiments.

3 Results

3.1 Morphology of cerebral endothelial cells

Living cells are inhomogeneous structures, neither spatial nor temporal elasticity is constant. AFM was used to investigate morphology and elasticity of CECs by performing high-resolution images and SCFS as complementary technique to examine their elasticity.

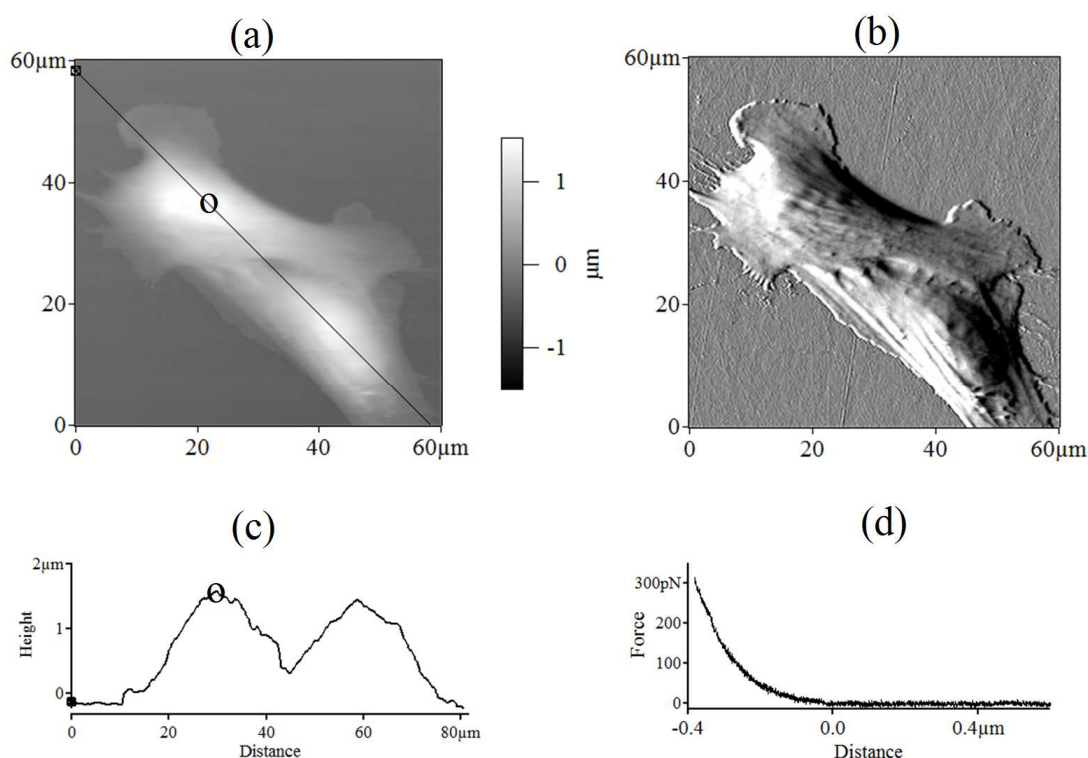


Figure 5. AFM image of sub-confluent cerebral endothelial cells: (a) height image of two cells in contact; (b) the amplitude (error signal) image; (c) height profile along the line shown on panel (a); (d) trace (approach part) of single force curve measured over nucleus at point marked with “o” on panel (a) and (c).

Three different cell culture stages were investigated and compared: the first being sparsely plated, the second totally confluent while the third being confluent and fixed with 4% paraformaldehyde. In each case, beside morphology, the spatio-temporal elasticity was monitored.

Figure 5 shows an image of sparsely plated living endothelial cells. The amplitude image on panel b, is more sensitive to small surface details. Two interconnected cells with

overlapping regions can be seen, with their nuclei emerging at the center. Lamellipodia can be identified as large cytoskeletal projections towards the leading edge of the cell. These are thought to be the motors of motile cells as they try to establish new connections, and junctions with each other. Beside this, parts of the cytoskeletal structure are observable, as long lines along the cell axis. As the section reveals (Figure 5, panel c), cells are few micron high, with a maximum, mainly at their nuclei region.

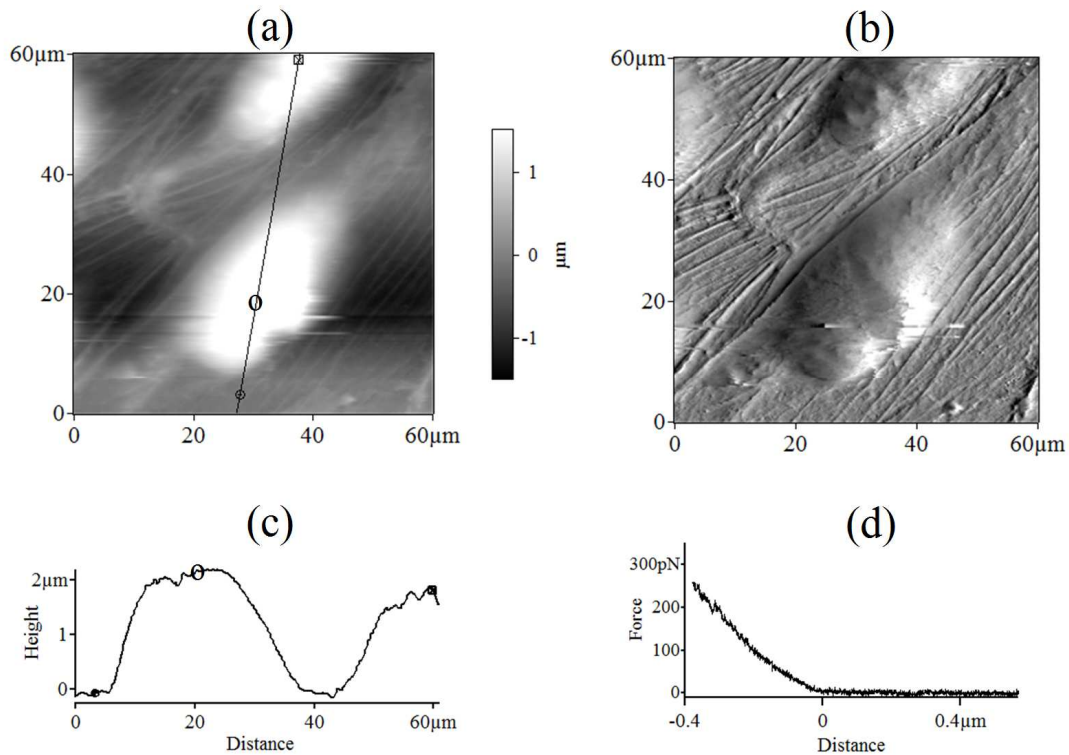


Figure 6. AFM image of a confluent cerebral endothelial cell culture. Conditions on panels (a-d) are similar to that on Figure 5, correspondingly.

The confluent living cell culture (Figure 6) revealed more details, which are highlighted by the error image (Figure 6, panel b). A flat portion of the cell, richly interlocked by filamentous cytoskeletal structures, surrounds the smooth nuclear part.

Their height is larger compared to the sub-confluent ones. Due to the lack of free Petri dish surface, only the level difference between the flat part of the cell and the nucleus can be measured, which is more than two microns (Figure 6, panel c). The real height of the cell is actually larger. Due to contact inhibition, CECs *in vitro* form a tight monolayer with 1-3 micrometer thickness. At the border of two adjacent cells, intercellular connections are clearly visible. Here the cells are highly connected by intercellular junctions, which are complex structures linked to cytoskeletal network.

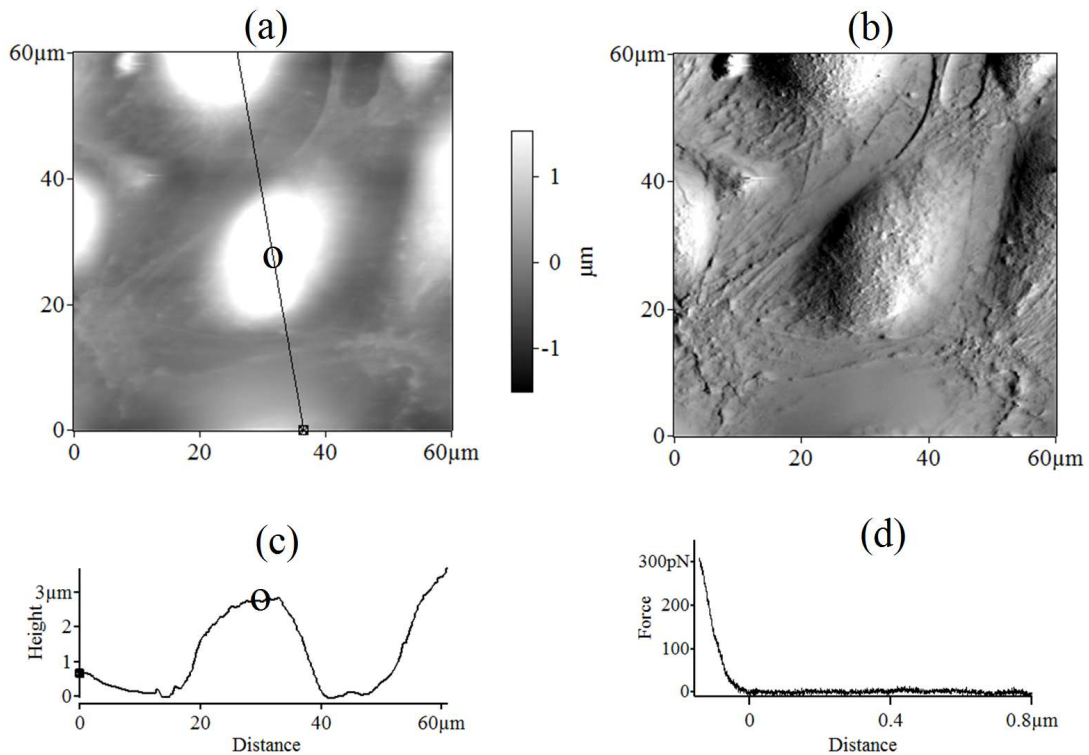


Figure 7. AFM image of a confluent fixed cerebral endothelial cell culture. Conditions on panels (a-d) are similar to that on Figure 5, correspondingly.

After fixating the totally confluent cell culture with paraformaldehyde, dramatic changes could be observed on the AFM image (Figure 7, panel a, b), compared to living confluent ones (Figure 6, panel a, b).

The junctional regions of the cells can be still identified, while the cytoskeletal structure suffered considerable alterations. Traces of cytoskeletal filamentous networks still can be distinguished; however, the cell surface became rougher. This might be due to small membrane protrusions as well as aggregation or cross linking of glycocalyx components. Apparent cellular height at region of nuclei became even larger, as it is depicted on Figure 7, panel c.

3.2 Elasticity of cerebral endothelial cells

Considering the force curves (Figure 5, Figure 6, Figure 7, panel d) obtained roughly at the middle of the cell, the elasticity of the three different cultures was estimated. While the sub-confluent and confluent cells share the same range of elasticity, the values for the fixed cells increased with one order of magnitude. This high value reflects very well the effect of protein cross-linking, due to paraformaldehyde, which

stabilizes the cellular structures. Although this fixation method might be considered as a gentle one, notable structural changes arose upon its application. This implies the need of elevated prudence and attentiveness, while investigating fixed cell cultures.

3.2.1 Spatial elasticity

Elasticity measurements, for spatial distribution, were effectuated along the lines drawn on images (Figure 5, panel a; Figure 6, panel a; Figure 7, panel a). At each

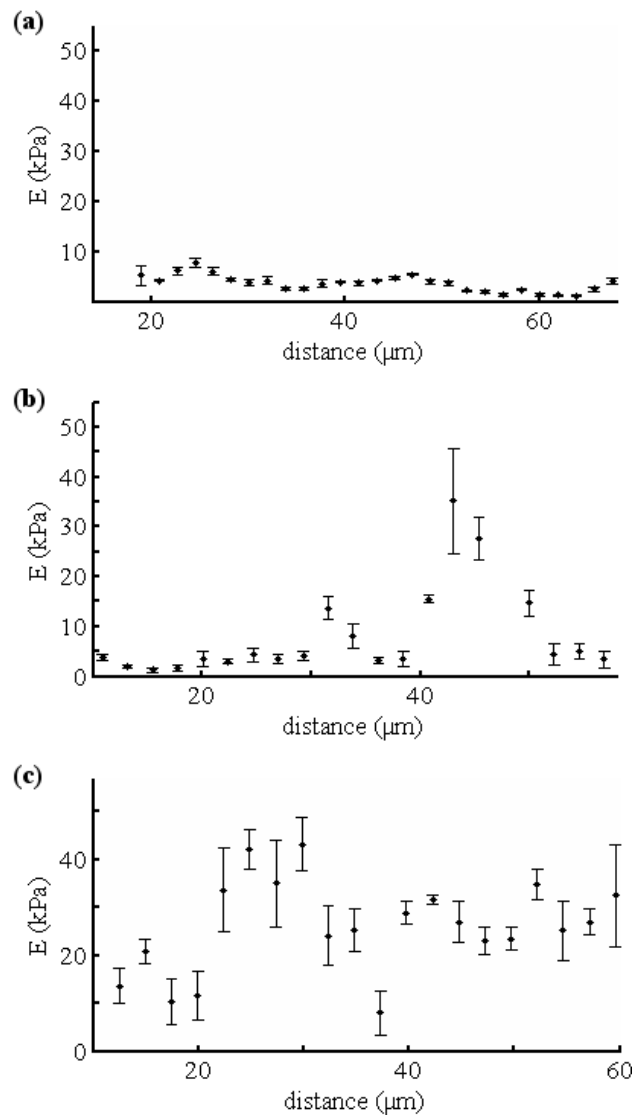


Figure 8. Spatial dependence of endothelial cells elasticity. Panels show different endothelial culture stages: (a) living sub-confluent, (b) living confluent, (c) fixed confluent. Points represent average \pm standard deviation, calculated from five consecutive forces

individual measuring point five consecutive forces were recorded. The calculated values of YM, for each of the culture stages mentioned in previous section, are depicted by Figure 8.

The spatial dependence of elasticity of the isolated cells showed an increase toward the periphery (Figure 8, panel a) with the value of the Young's modulus increased by few fold. The confluent cells showed the same tendency, but in a much larger extent (Figure 8, panel b). Here, increase of the Young's Modulus is roughly one order of magnitude. Stiffening at periphery could be caused by the appearance and localization of intercellular junction proteins.

Unfortunately, the error of the measurements increases too, as the indentation curve becomes steeper. On fixed culture no change could be observed in the elasticity between the central and peripheral region. The Young's Modulus is uniformly large

and fluctuates across the whole cell (Figure 8, panel c). This could be due to the paraformaldehyde treatment, which cross-binds proteins in the cell, resulting in roughly uniform elasticity.

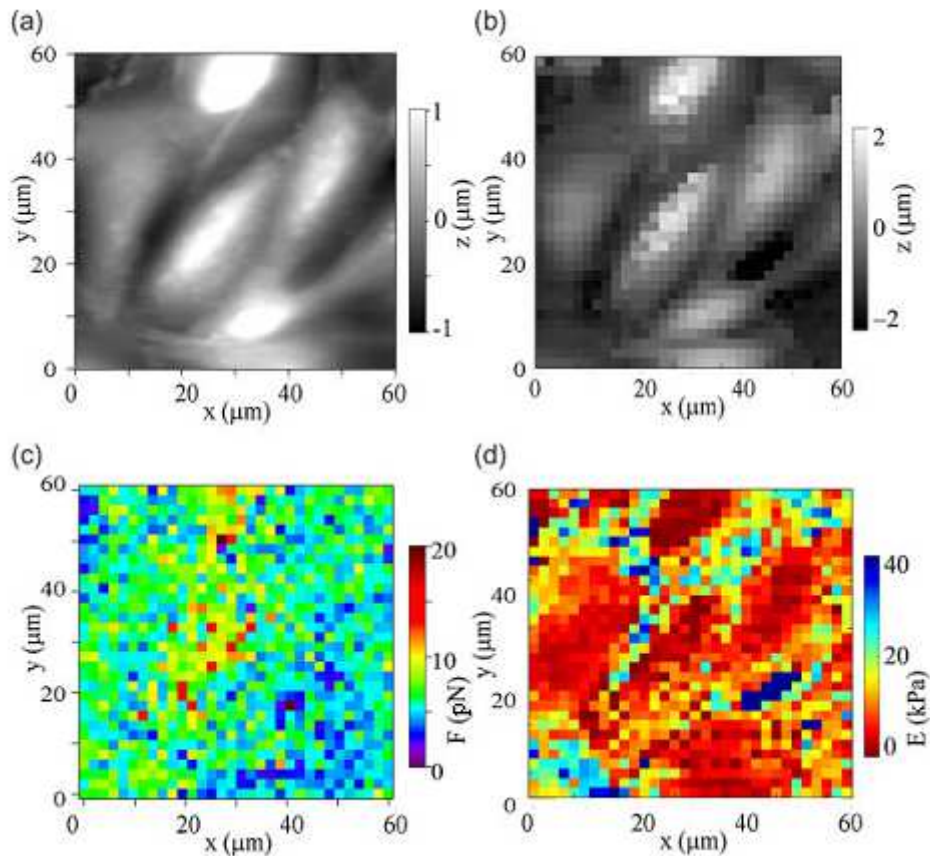


Figure 9. Force Volume Mapping of living confluent endothelial cells. (a) recorded height image prior to mapping, (b) height reconstructed from force curves, (c) adhesion map, (d) elasticity map.

On confluent cells force-volume elasticity mapping was performed too (Figure 9) which corroborated with the finding that the cells are more rigid at the periphery. Although this type of measurement is rather rich in information, it cannot be done frequently because the large number of force measurements effectuated over the whole studied surface might harm the cells. The edges were stiffer, probably because the accumulation of tight and adherent junction proteins.

3.2.2 Temporal elasticity

On cerebral endothelial cells the temporal dependence of the elasticity was measured over the nuclear region, which is the most insensitive to small position shifts.

Despite of an expected constant elasticity in case of sub-confluent and confluent cells, an attenuated oscillation was observed.

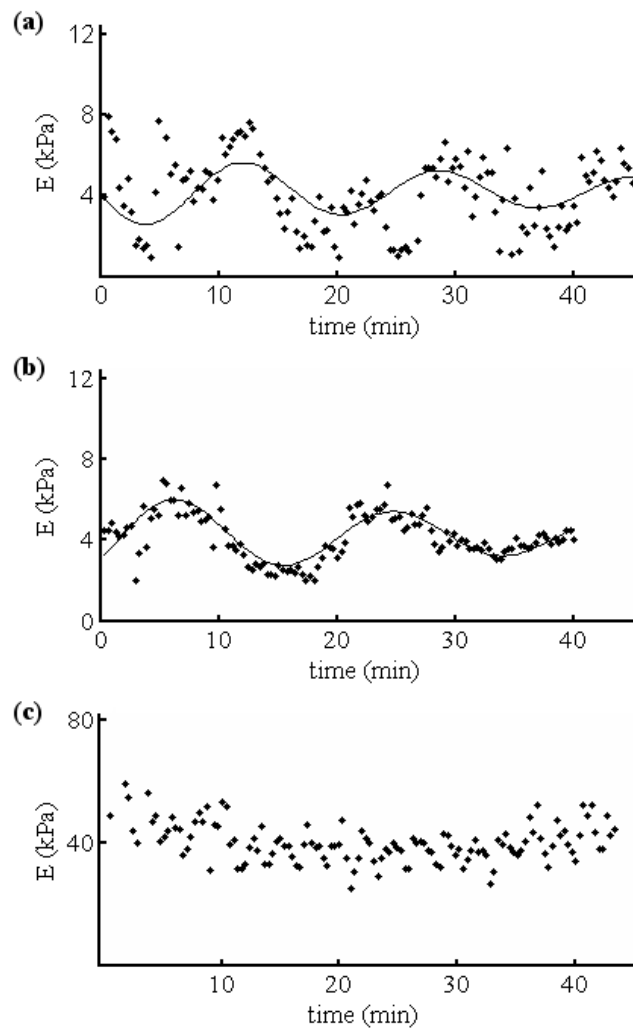


Figure 10. Elasticity in time of endothelial cells; (a): living sub-confluent, (b): living confluent, (c): fixed confluent cultures. Points are individual successive measurements at place denoted with o, on Figures 5-7 accordingly. Solid line is a slightly attenuated oscillation.

Dots are individual point of measure, while the solid line shows an attenuated oscillation. Two third of the measurements, repeated more than ten times, showed this oscillation, with a period of 10 to 20 minutes. However, in some cases a superposition of many oscillations showed up. On sub-confluent cells the oscillation period was around 15 minutes and the amplitude decreased in time (Figure 10, panel a). The confluent cells had a period of about 20 minutes and exhibited a faster attenuation of the oscillation, (Figure 10, panel b).

Fixed cells never showed this type of oscillation (Figure 10, panel c), proving that this phenomenon is feature, characteristic to living cells. The external conditions, which affect the amplitude, period and attenuation of the oscillations, are under debate.

3.3 Intercellular mechanics

The interaction between endothelial layer and individual melanoma cell, can be regarded as a model for primary steps of tumor cell transmigration. The appearance of adhesion between melanoma and endothelial cells as well as the relaxation upon applied mechanical pressure in function of load and time they spent in contact, was investigated. Adhesion force measurements were carried out with AFM, by pressing one cell to another and monitor the unbinding force upon retraction. (Schematic drawing of measurement setup can be found on Figure 4).

The two representation modes of the recorded signal (Figure 11) clearly show the two features of interest. The total adhesion force was calculated by taking the difference between the minimum of the retrace part and the average of last few points of the curve (Figure 11, panel a). For clarity, see schematic Figure 2, where total adhesion force is marked with “A”. The time dependent representation shows the relaxation decay during dwell time (Figure 11, panel b).

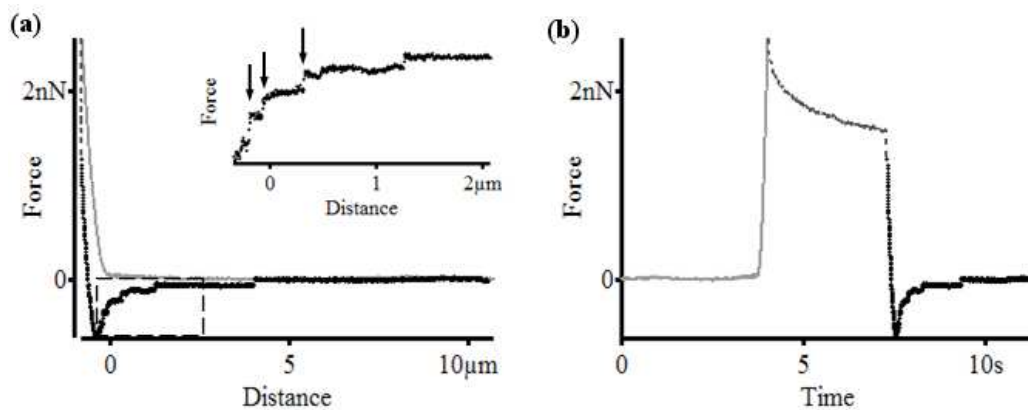


Figure 11. Force measurement effectuated with a melanoma cell bound to a tipless cantilever on a living confluent endothelial layer. The same curve shown: (a) force vs. distance, (b) force vs. time. Inset: Magnified view of area in dashed box. Arrows mark individual ruptures (jumps).

The dwell time is the extra period between the time point of reaching maximal load and the point of starting to pull back the cantilever. Schematic representation on Figure 2, marks the stress relaxation with “S”. Care should be taken not to confuse this with total contact time. Dwell time was chosen due to simplify the representations. Compared to the few ten seconds, the real contact time would be longer with one or maximum two seconds, however this would not alter the shown results.

Figure 12 reflects comparison of typical force curves taken on different surfaces: hard Petri surface probed with a bare tip (“A” lines), endothelial cells probed with bare tip (“D” lines), endothelial layer probed with living melanoma cell (“C” lines) and fixed endothelial layer probed with living melanoma cell (“B lines”).

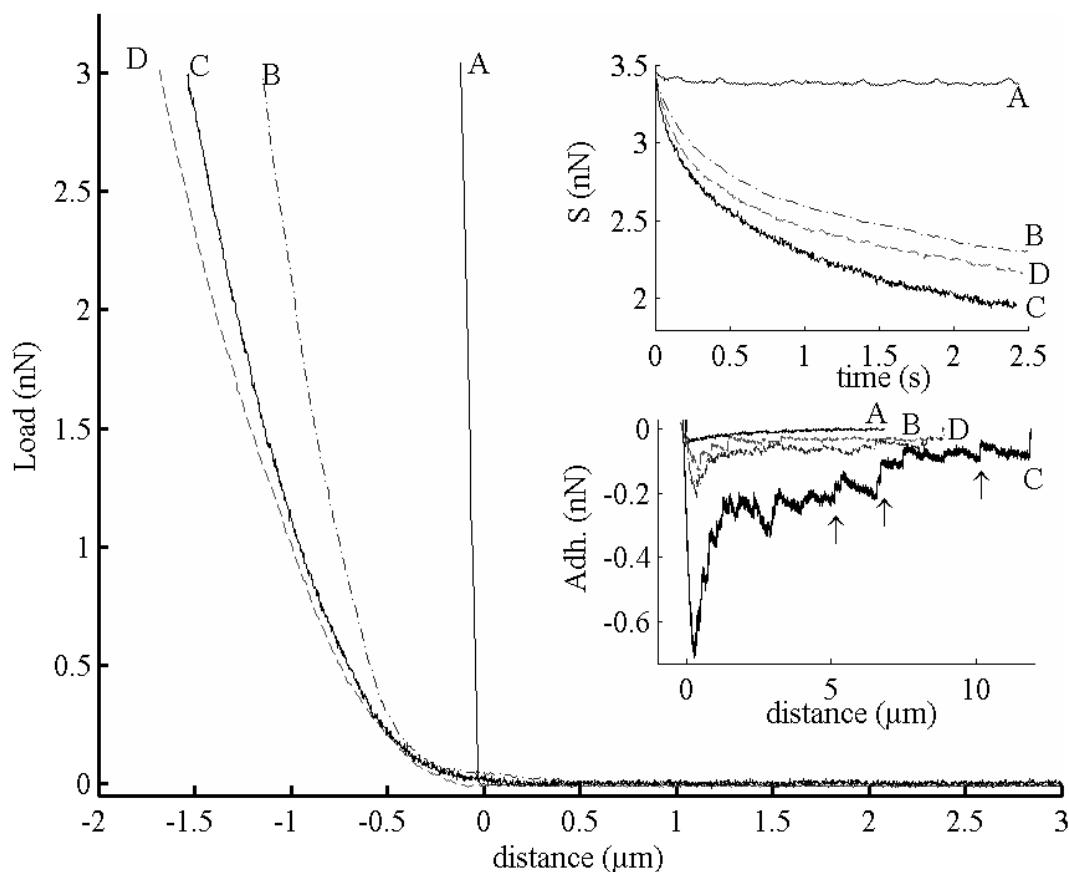


Figure 12. Comparison of different force curves representing the following sets: (A) Tip - Petri surface, (B) Melanoma cell - Fixed Endothelial cell, (C) Melanoma cell - Endothelial cell, (D) Tip - Endothelial cell. Stress relaxation (top inset) and adhesion forces (bottom inset) corresponding to each force curve. On the latter the arrows point to typical rupture like events.

The figure compares the elasticity of the above-mentioned stages. Unfortunately, only qualitative comparison is possible, as the parameters for different sets do not allow calculations mentioned at section 2.3.1. Cell fixation (line B) induces apparent stiffening compared to living cells (line C). The top inset, in Figure 12, shows the load dissipation in time, while the bottom inset compares the attractive forces measured for the above mentioned stages. The relaxation and adhesion present considerable correlation, suggesting that due to larger interacting areas higher affinity may be reached.

3.3.1 Adhesion

Between the melanoma “tip” and the cell free surface of the Petri dish, a small nonspecific adhesion (Figure 13, panel a) was observed. Changing the load force or the dwell time the change of the adhesion is within the error bars. In the case of confluent living endothelial cell layer, tested with a melanoma cell, the adhesion in function of dwell time shows saturation-like behavior (Figure 13, panel b). It seems that there is a limited amount of adhesion at a given load. As the load increases, the monitoring cell is pushed closer to the cell layer and the binding force increases as well. On the fixed cell layer, the intercellular adhesion force is much weaker (Figure 13, panel c), but still larger than nonspecific adhesion depicted on panel a, Figure 13.

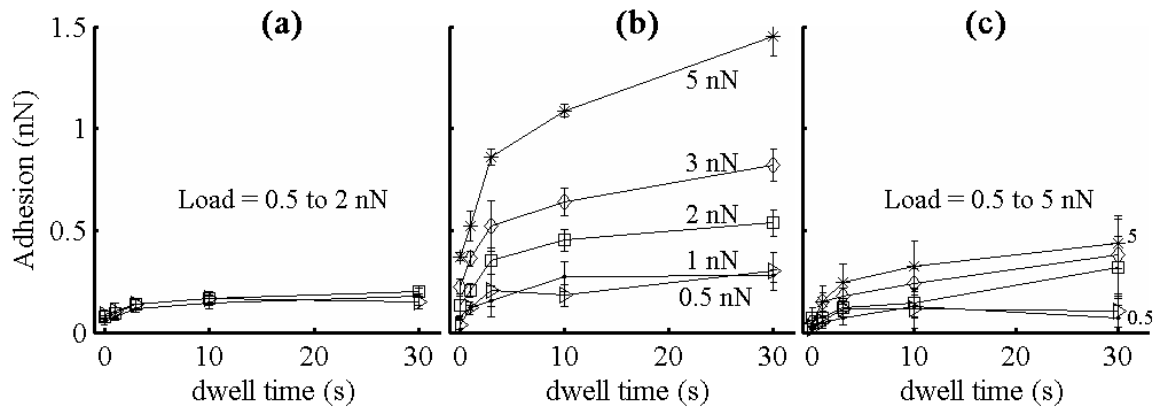


Figure 13. Change in intercellular adhesion as a function of dwell time under constant load. The tested surface was: (a) Petri dish, (b) living endothelial cells, (c) fixed endothelial layer

The adhesion force measured on living cells showed stair like ruptures during contact break up in the retrace phase of the force curve. On Figure 12 (bottom inset) these are pointed out by small arrows. These jumps correspond to the rupture of the binding between the melanoma cell and the endothelial layer. With a home-developed MATLAB protocol, the curves were analyzed by searching for and identifying of the individual rupture events. Total rupture number and size was calculated and plotted against dwell period (Figure 14).

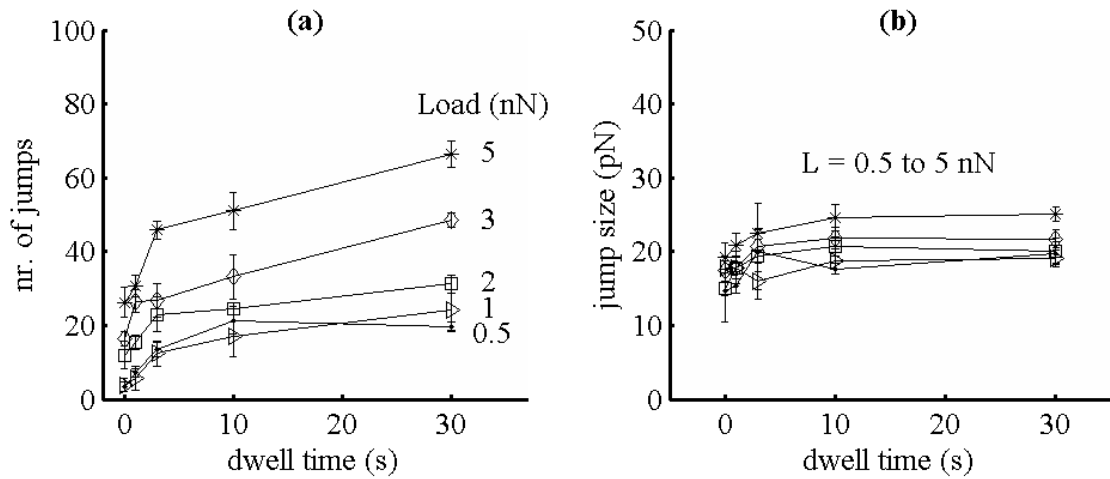


Figure 14. Number of individual adhesion jumps (a) and their size (b) in function of applied load.

The number of jumps showed saturation-like increase in function of dwell time (Figure 14 a). The jump size distribution showed almost no variance giving the minimal jump size an average of about 20 ± 5 pN (Figure 14, panel b). The correlation of these data with total adhesion force is remarkable.

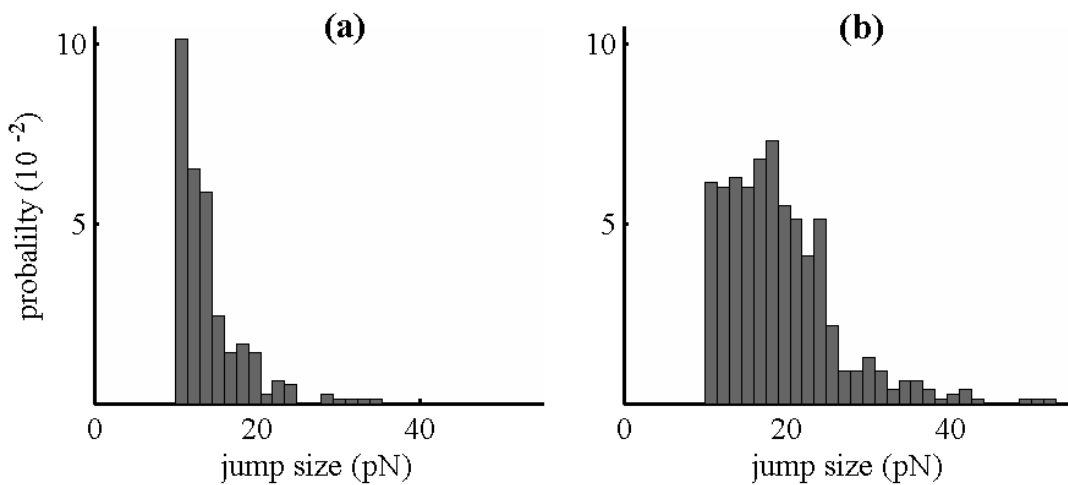


Figure 15. Histogram of jump (rupture) size distribution: between living melanoma and fixed endothelial layer (a); between living melanoma and living endothelial cells (b).

A histogram the individual stair-like rupture occurrences of living endothelial cells probed with melanoma cell, show a clear maximum at 20 pN (Figure 15, panel b). Moreover, higher values appear at 40 pN. The jump frequency on fixed endothelial layer is shifted towards 10 pN (Figure 15, panel b), which is close to the defined calculation threshold (see section 2.3.3 for details). The adhesion between the two cells is altered, but the origin of adhesion is still blurred.

3.3.2 Stress relaxation

Upon mechanical stimulation, cellular components need to withstand and adapt. This kind of flexibility is the result of both membrane and cytoskeletal reorganization, ruled by viscoelastic properties. Stress relaxation, the rearrangement of the sample at constant load arises if the indenter holds still some time before retraction.

By holding still the position of the vertical actuator after the preset load is reached, equilibrium of the system occurs, which is the decay in time of the applied stress. Relaxation of a single cell upon mechanical stress can be described by a two-component viscoelastic model applied for cells. Our data, recorded with a cell “probe”, shows similar decay. Two different but simultaneous processes can be clearly distinguished by fitting the relaxation data with the sum of two exponents. In case of tip-cell stress relaxation these two processes are thought to be the results of membrane dislocation, and cytoskeletal reorganization. However, in our case only a presumption-like assignment can be made to each participating cell.

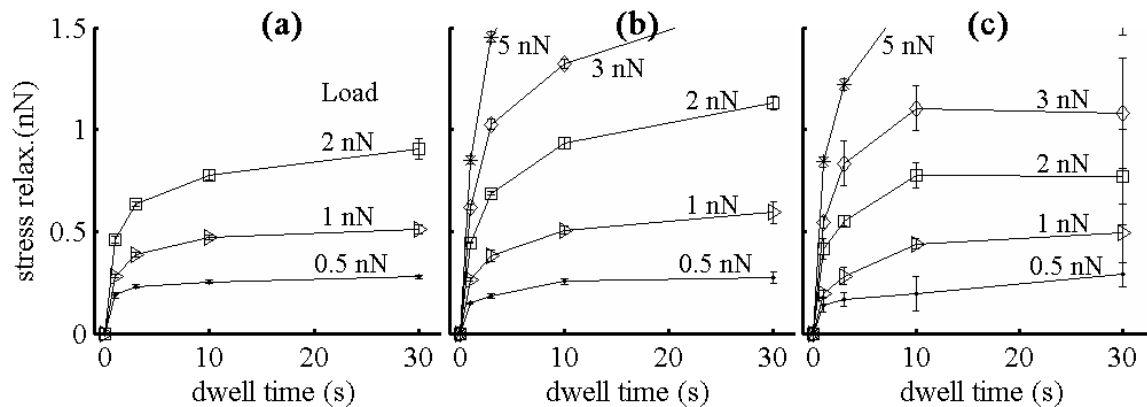


Figure 16. Change in stress relaxation as a function of dwell time under constant load. The supported surface was: (a) Petri dish, (b) living endothelial cells, (c) fixed endothelial layers

During the measurements a bare tip examines living endothelial cell layer at first. Small rearrangement of the sample occurs which manifests in the fact that the trace and retrace curves presented in function of distance do not overlap (Figure 11, panel a). Representing the force against elapsed time the effect of plastic deformation is clearly visible (Figure 11, panel b). The stress applied on the cell by the load force is partially relaxed by rearrangement of the contacting surface and cytoplasmic components of the cell.

Next, a melanoma cell was bound to a tipless cantilever and used as the probe. By comparing ‘Figure 16 a’ and ‘Figure 16 b’ it can be seen that the interaction between the

cells produces large stress relaxation. The living and paraformaldehyde fixed cells measured in the same condition (Figure 16 b, c) showed larger relaxation boundaries but qualitatively a same pattern. Data was extracted with the routine described at chapter 2.3.4.

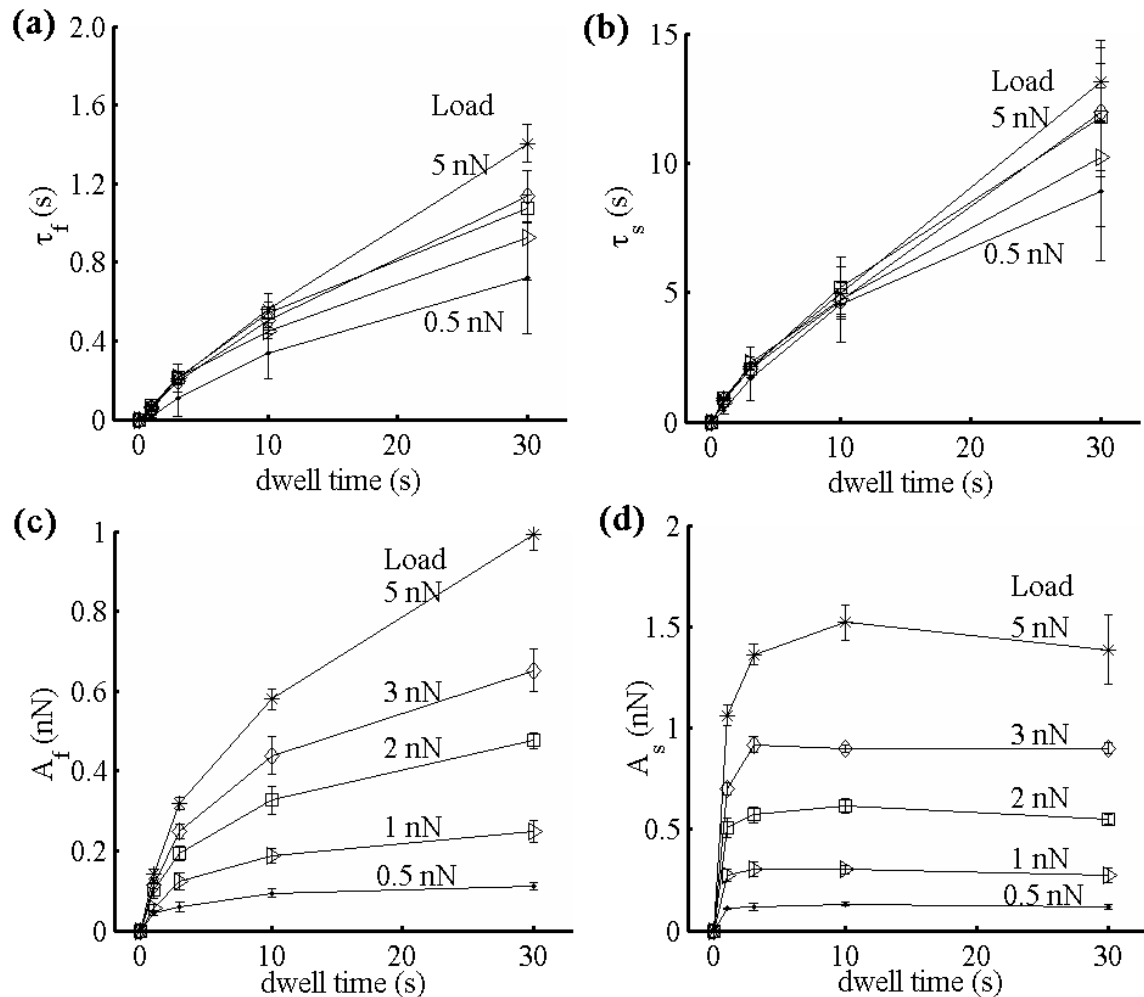


Figure 17. Lifetime and amplitude of stress relaxation measured between living melanoma and endothelial cells. (a) and (c) show the components of the fast while (b) and (d) shows the components of slow exponentials.

Figure 17 Shows the lifetime and amplitude of stress relaxation plotted against dwell time, for different loading forces. Indices show the distinction between slow (s) on panel a and c. Fast (f) components on panel b and d. Lifetime does not reach saturation, while amplitude clearly show this pattern. Amplitude of slow exponential is practically independent of dwell time, while the lifetimes are independent of applied load.

4 Discussion

4.1 Heterogeneities in spatio-temporal elasticity of cerebral endothelial cells

Cellular elasticity has been under constant debate during the last few decades. Aiding this debate, biomechanics has become a still enlarging multidisciplinary and complementary field for medicine and life sciences. Development of technical and instrumental support has led to better understanding and description of cell biology. Hence, cellular biomechanics is an important and promising field not only for broadening our knowledge, but also for counteracting many pathological processes.

As it becomes widely accepted that living cells are not water filled balloons, more and more aspects of cell biology, cell mechanics get scientific attention. Living cells do maintain active molecular traffic with their environment, which implies continuous adaptation and changes in time and space.

Endothelial cells have to continuously withstand mechanical forces upon blood shear (Butler et al. 2001) and red blood cell pressure. Their biomechanical investigation could lead to promising solutions for several disorders.

Studying the spatial and temporal elasticity of living cerebral endothelial cells, three different culture types were monitored and presented: sub-confluent, confluent and fixed confluent. These stages might be considered as stages of wound healing models, except the last one, which was introduced as an internal control. Wound healing related studies report changes in epithelial cell elasticity during their migration, showing an elasticity increase with wound edge distance (Wagh et al. 2008). Comparing panels a and b on Figure 8, confluent cells appear a bit harder at perinuclei regions what is not contradictory with previously cited results, however, those were epithelial cells. Paraformaldehyde fixation induces remarkable hardening as is plotted on panel c, Figure 8. At least one order of magnitude increase in YM occurs upon fixation, not to mention the spatial inhomogeneities from point to point.

Cell shape and elasticity depend on cytoskeletal networks and contractile systems (Levayer and Lecuit 2012), and external factors surely influence cell stiffness as well (Yang et al. 2012). Water soluble salts do have considerable influence on endothelial cell

stiffness (Oberleithner et al. 2009; Oberleithner et al. 2007), not to speak of osmotic parameters (Bálint et al. 2007a). As our experiments were carried out in Leibovitz medium, pH and concentration shifts can be excluded. Medium change and addition of external factors were not applied.

Analyzing temporal elasticity of CECs one common thing occurred during measurements: fixation causes hardening as plotted on panel c, Figure 10. As the panel a and b show on the same figure, elasticity of sub-confluent and totally confluent CECs, are far not constant in time. Moreover, under certain conditions it shows periodic oscillations, which in case of the confluent culture appears to be the most straightforward (Figure 10, panel b). The correlation between the attenuated oscillation (solid line) and measured values (dots) is remarkable.

Unfortunately the exact triggers of these oscillation-like alterations is still blurred, but some parameters can be excluded definitively. Apoptotic properties need to be taken into consideration (Pelling et al. 2009), however, different images were made prior and after time laps force measurements, and no changes were detected neither in morphology, nor in spatial manner. In addition to this, the cells were selected randomly and it is very unlikely that most of them were in apoptotic phase. Temporal dependence might be temperature dependent (Sunyer et al. 2009), but, the temperature change during experiments was under half a degree Celsius. This would not induce the level of changes observed. It might be age dependent (Lieber et al. 2004), nevertheless, on this time scale, direct connections cannot be made. Spreading HUVEC cells were reported to have morphology correlated stiffness (Stroka and Aranda-Espinoza 2011). Unfortunately, based on this study, it is difficult to draw valuable conclusions regarding our case, as in their experiments the cells were gently fixed. Additionally, depth dependence of elastic modulus might induce few fold changes (Pogoda et al. 2012), but here is not the case, as experiments were made with constant indentation depth.

Applied forces induce mechanotransduction, which propagates through stress fibers (Lu et al. 2008; Rosenbluth et al. 2008). Involvement of contractile systems and cytoskeletal reorganization is inevitable. Oscillating elasticity in correlation with myosin activity was reported, with one order of magnitude shorter time period (Schillers et al. 2010), however, due to lack of additional chemical agents at this time point either direct, or indirect connections would be only speculative.

4.2 Insights into intercellular mechanics of endothelial cell layer tested with melanoma cell as a probe

Living cells not only sense but actively exert forces on both intra and extracellular environment (Discher et al. 2005; Tan et al. 2003). Intercellular adhesion is involved in many inflammatory and pathologic processes (Abu-Lail and Camesano 2003; Almqvist et al. 2004; Liu et al. 2010; McGettrick et al. 2009; McNamee et al. 2006), and represents an important aspects in many other phenomena (Sheng et al. 2007). AFMs are outstanding at monitoring these forces between cell and substrate or arbitrary cells.

Similar to leukocyte-endothelial binding (Zhang et al. 2003), SCFS was applied to measure total adhesion force between a single living malign cell and living endothelial layer. Dependence of adhesion and stress relaxation on dwell time at different load forces was measured. A small nonspecific adhesion exists between the melanoma “tip” and the Petri dish surface practically independent of load strength and time lapsed (Figure 13, panel a). In the case of confluent living endothelial cell layer, tested with a melanoma cell, the adhesion in function of dwell time shows saturation-like behavior (Figure 13, panel b). It seems that there is a limited number of binding at a given load force. With the increase of the load the binding force increases too, while the monitoring cell is pushed closer to the cell layer. This might be the effect of increase in the number of binding elements or in the individual binding forces. In case of the fixed cell layer the adhesion force is much weaker (Figure 13, panel c).

Many ligand-receptor studies have successfully reported intercellular, or intermolecular characterizations (Robert et al. 2008). Valuable data can be obtained from retraction of the two sides regarding size and number of occurred individual rupture events. In our study, the intercellular adhesion showed stair-like ruptures (jumps) during the retraction (retrace) phase of the force curve. These correspond to the rupture of the binding between the melanoma cell and the endothelial cell covered surface, since in other cases they practically do not occurred (Figure 12, bottom inset).

By enumerating the individual de-adhesion events, a low-end estimation of the number of active intercellular adhesion molecules can be made. Load dependent rupture number showed saturation like increase in function of dwell time (Figure 13, panel a). Average rupture size was blurred by seldomly occurring large values which led to

deviation increase, shown on Figure 13, panel b. Blocking one side by fixation of the endothelial layer the total adhesion is almost inhibited (Figure 13, panel c).

Both, the number and size of ruptures decreased. Showing the total rupture frequency on a histogram, the minimal rupture size value resulted in 20 pN (Figure 15, panel b). Cadherin mediated adhesion on chinese hamster ovary cell (CHO) (Panorchan et al. 2006; Zhang et al. 2009) and in single molecule spectroscopy (Zhang et al. 2009) was reported to have similar results. Slightly higher values were reported for α -Catenin mediated E-cadherin-dependent adhesion on wild type CHO cells (Bajpai et al. 2008). It is hard to determine the exact type of molecules involved, as multiple simultaneous event occurrences and low specificity may alter the results.

The presented cell adhesion measurements monitor quick individual processes of initial adhesion at single molecule level. Therefore, it can be regarded as a model for first step of cellular transmigration. After the established contact, almost Hookean cell stretching takes place until the maximum load is reached. This induces several accommodation processes involving membrane and cytoskeletal reorganization in order to regain the equilibrium. Mechanical relaxation upon applied load (stress) was monitored between living melanoma and endothelial layer. Stress relaxation parameters could have important aspects reflecting metastatic potential of malignant cells (Darling et al. 2007; Moreno-Flores et al. 2010a).

Total stress relaxation force in function of dwell time showed very similar behavior (Figure 16 a-c) to maximal adhesion. It cannot be distinguished the cell free surface from the living cell or fixed cell covered surfaces. As two individual cells are involved in this process, based on viscoelastic theory (Moreno-Flores et al. 2010b), four different relaxation process would contribute to overall response. Surprisingly, a biexponential fit satisfies the measured data. Apparently the tip-bonded cell has the dominant role in mechanical relaxation.

The stress relaxation curves were fitted with a biexponential curve. The lifetime of the exponents were roughly independent from the load force, as it was found in case of breast cancer cells (Moreno-Flores et al. 2010a) too. Presented in function of dwell time the lifetimes of both the fast and slow components showed a weak linear dependency (Figure 17, panel a, b). The amplitude in both cases showed saturation like behavior (Figure 17, panel c, d).

Three different surfaces were compared: cell free, confluent CEC layer, and fixed CEC layer. The three different surfaces showed no remarkable difference at the level of individual relaxation components, just as in case of the total relaxation amplitude. The dominance of the probe cell is obvious (Figure 16), however influence of the opposite side might be important in some cases.

5 Summary

This study presents insights into mechanobiology of cerebral endothelial cells, which form the morphological basis of the BBB.

First, morphological and elastic characterizations of three different endothelial cell stages are presented. Sub-confluent, totally confluent and fixed confluent cultures were compared. High-resolution images revealed highly organized cytoskeletal network of confluent layer, extruding lamellipodia of sub-confluent cells and rougher membrane rheology of fixed confluent layer.

Distribution of elastic modulus was measured over different cellular components, followed by a time-lapse monitoring of the nuclei's YM. The nuclear region appeared to be softer and less sensitive on testing positions, while towards the periphery a considerable increase of the elastic modulus was registered. Additionally, sub-confluent cells tend to be overall softer, even at peripheral regions. Fixed cell culture showed elevated YM values, over one order of magnitude, regardless of testing position. The time-lapse elasticity showed attenuated oscillations both on sub-confluent and totally confluent cultures. This is characteristic of living cells since fixed cultures were not showing this feature. Orchestrated cytoskeletal dynamics can produce similar oscillations. Its exact origin is still under debate, however the possibility that it is a response of the cell to the external stimuli, cannot be excluded.

To model the first step of cellular transmigration, living monolayer of endothelial cells was tested with a living melanoma cell as a probe. These results are presented in second part. Two features of force spectroscopy were studied, the intercellular adhesion force and relaxation upon mechanical stress. Their dependence on load and dwell time characterized the interaction between the monitored surfaces. The adhesion force was decomposed to small stair-like ruptures, having the elementary size of about 20 pN. Saturation on load and dwell time suggests that the adhesion force builds up as the sum of many elementary bindings.

Mechanical relaxation during sudden cell-cell contact was measured too. Total relaxation force recorded for different load saturated within seconds. Surprisingly, relaxation curves showed biexponential viscoelastic decay. Individual elements were calculated and compared on different combinations of cell-cell contact. The independence

of relaxation amplitude on the different tested surfaces suggests the dominance of the probe cell in this phenomena.

In this work we presented possibilities and advantages of AFM in live cell imaging and single cell force spectroscopy. The ability to work in liquid environment at human body temperature, offers the favor to record accurate and nanoscale precision data on mechanical properties of different biomaterials.

From the above-mentioned observations, we conclude that with help of these parameters, insights can be gained into biomechanics of BBB-forming brain endothelial cells. These findings might contribute to better characterization and description of live cell responses on mechanical stimuli, what is important component e.g. in angiogenesis. Analysis on cell-cell adhesion and mechanical relaxation might provide valuable data for cell adhesion related pathologies or research of metastatic cell migration.

6 References

Abu-Lail NI, Camesano TA (2003) Role of ionic strength on the relationship of biopolymer conformation, DLVO contributions, and steric interactions to bioadhesion of *Pseudomonas putida* KT2442. *Biomacromolecules* 4:1000-1012. doi: 10.1021/bm034055f

Albuquerque ML, Waters CM, Savla U, Schnaper HW, Flozak AS (2000) Shear stress enhances human endothelial cell wound closure in vitro. *Am J Physiol Heart Circ Physiol* 279:H293-302.

Almqvist N, Bhatia R, Primbs G, Desai N, Banerjee S, Lal R (2004) Elasticity and adhesion force mapping reveals real-time clustering of growth factor receptors and associated changes in local cellular rheological properties. *Biophys J* 86:1753-1762. doi: 10.1016/S0006-3495(04)74243-5

Ando T, Uchihashi T, Kodera N, Yamamoto D, Miyagi A, Taniguchi M, Yamashita H (2008) High-speed AFM and nano-visualization of biomolecular processes. *Pflugers Arch* 456:211-225. doi: 10.1007/s00424-007-0406-0

Anor T, Grinberg L, Baek H, Madsen JR, Jayaraman MV, Karniadakis GE (2010) Modeling of blood flow in arterial trees. *Wiley Interdiscip Rev Syst Biol Med* 2:612-623. doi: 10.1002/wsbm.90

Azeloglu EU, Costa KD, 2011. Atomic Force Microscopy in Mechanobiology: Measuring Microelastic Heterogeneity of Living Cells. In: Braga, P.C., Ricci, D. (Eds.) *Atomic Force Microscopy in Biomedical Research: Methods and Protocols*. Springer, Springer Protocols, pp. 303-329

Bajpai S, Correia J, Feng Y, Figueiredo J, Sun SX, Longmore GD, Suriano G, Wirtz D (2008) α -Catenin mediates initial E-cadherin-dependent cell-cell recognition and subsequent bond strengthening. *Proc Natl Acad Sci U S A* 105:18331-18336. doi: 10.1073/pnas.0806783105

Bálint Z, Krizbai IA, Wilhelm I, Farkas EA, Párducz Á, Szegletes Z, Váró G (2007a) Changes induced by hyperosmotic mannitol in cerebral endothelial cells: an atomic force microscopic study. *European Biophysical Journal* 36:113-120.

Bálint Z, Nagy K, Laczkó I, Bottka S, Végh GA, Szegletes Z, Váró G (2007b) Adsorption and Self-Assembly of Oligodeoxynucleotides onto a Mica Surface. *Journal of Physical Chemistry C* 111:17032-17037.

Bálint Z, Végh AG, Popescu A, Dima M, Ganea C, Váró G (2007c) Direct Observation of Protein Motion during the Photochemical Reaction Cycle of Bacteriorhodopsin. *Langmuir* 23:7225-7228.

Benoit M, Selhuber-Unkel C, 2011. Measuring Cell Adhesion Forces: Theory and Principles. In: Braga, P.C., Ricci, D. (Eds.) *Atomic Force Microscopy in Biomedical Research.* , Springer Protocols, pp. 355-377

Binnig G, Quate CF, Gerber C (1986) Atomic force microscope. *Phys Rev Lett* 56:930-933.

Bozic KJ, Browne J, Dangles CJ, Manner PA, Yates AJ,Jr, Weber KL, Boyer KM, Zemaitis P, Woznica A, Turkelson CM, Wies JL (2012) Modern metal-on-metal hip implants. *J Am Acad Orthop Surg* 20:402-406. doi: 10.5435/JAAOS-20-06-402

Buckley CD, Rainger GE, Bradfield PF, Nash GB, Simmons DL (1998) Cell adhesion: more than just glue (review). *Mol Membr Biol* 15:167-176.

Burr DB (2011) Why bones bend but don't break. *J Musculoskelet Neuronal Interact* 11:270-285.

Butler PJ, Norwich G, Weinbaum S, Chien S (2001) Shear stress induces a time- and position-dependent increase in endothelial cell membrane fluidity. *Am J Physiol Cell Physiol* 280:C962-9.

Carl P, Schillers H (2008) Elasticity measurement of living cells with an atomic force microscope: data acquisition and processing. *Pflugers Arch* 457:551-559. doi: 10.1007/s00424-008-0524-3

- Coles JM, Blum JJ, Jay GD, Darling EM, Guilak F, Zauscher S (2008) In situ friction measurement on murine cartilage by atomic force microscopy. *J Biomech* 41:541-548. doi: 10.1016/j.jbiomech.2007.10.013
- Cross SE, Jin YS, Rao J, Gimzewski JK (2007) Nanomechanical analysis of cells from cancer patients. *Nat Nanotechnol* 2:780-783. doi: 10.1038/nnano.2007.388
- Darling EM, Zauscher S, Block JA, Guilak F (2007) A thin-layer model for viscoelastic, stress-relaxation testing of cells using atomic force microscopy: do cell properties reflect metastatic potential? *Biophys J* 92:1784-1791. doi: 10.1529/biophysj.106.083097
- Darling EM, Zauscher S, Guilak F (2006) Viscoelastic properties of zonal articular chondrocytes measured by atomic force microscopy. *Osteoarthritis Cartilage* 14:571-579. doi: 10.1016/j.joca.2005.12.003
- Davis ZJ, Abadal G, Hansen O, Borise X, Barniol N, Perez-Murano F, Boisen A (2003) AFM lithography of aluminum for fabrication of nanomechanical systems. *Ultramicroscopy* 97:467-472. doi: 10.1016/S0304-3991(03)00075-5
- Deckert-Gaudig T, Deckert V (2011) Nanoscale structural analysis using tip-enhanced Raman spectroscopy. *Curr Opin Chem Biol* 15:719-724. doi: 10.1016/j.cbpa.2011.06.020
- Discher DE, Janmey P, Wang YL (2005) Tissue cells feel and respond to the stiffness of their substrate. *Science* 310:1139-1143. doi: 10.1126/science.1116995
- Docheva D, Padula D, Popov C, Mutschler W, Clausen-Schaumann H, Schieker M (2008) Researching into the cellular shape, volume and elasticity of mesenchymal stem cells, osteoblasts and osteosarcoma cells by atomic force microscopy. *J Cell Mol Med* 12:537-552. doi: 10.1111/j.1582-4934.2007.00138.x
- Dulinska I, Targosz M, Strojny W, Lekka M, Czuba P, Balwierz W, Szymonski M (2006) Stiffness of normal and pathological erythrocytes studied by means of atomic force microscopy. *J Biochem Biophys Methods* 66:1-11. doi: 10.1016/j.jbbm.2005.11.003
- Fels J, Callies C, Kusche-Vihrog K, Oberleithner H (2010) Nitric oxide release follows endothelial nanomechanics and not vice versa. *Pflugers Arch* 460:915-923. doi: 10.1007/s00424-010-0871-8

- Fletcher DA, Mullins RD (2010) Cell mechanics and the cytoskeleton. *Nature* 463:485-492. doi: 10.1038/nature08908
- Franz CM, Puech P- (2008) Atomic Force Microscopy: A Versatile Tool for Studying Cell Morphology, Adhesion and Mechanics. *Cell Mol Bioeng* 1:289-300. doi: 10.1007/s12195-008-0037-3
- Gad M, Itoh A, Ikai A (1997) Mapping cell wall polysaccharides of living microbial cells using atomic force microscopy. *Cell Biol Int* 21:697-706. doi: 10.1006/cbir.1997.0214
- Greenwood J, Heasman SJ, Alvarez JI, Prat A, Lyck R, Engelhardt B (2011) Review: leucocyte-endothelial cell crosstalk at the blood-brain barrier: a prerequisite for successful immune cell entry to the brain. *Neuropathol Appl Neurobiol* 37:24-39. doi: 10.1111/j.1365-2990.2010.01140.x; 10.1111/j.1365-2990.2010.01140.x
- Hanna S, Etzioni A (2012) Leukocyte adhesion deficiencies. *Ann N Y Acad Sci* 1250:50-55. doi: 10.1111/j.1749-6632.2011.06389.x; 10.1111/j.1749-6632.2011.06389.x
- Hertz H (1882) Ueber die Berührung fester elastischer Körper. *Journal Für Die Reine Und Angewandte Mathematik* 1882:156-171.
- Hochmuth RM (2000) Micropipette aspiration of living cells. *J Biomech* 33:15-22.
- Hutter JL, Benchhoefer J (1993) Calibration of atomic-force microscope tips. *Review of Scientific Instruments* 64:1868-1873. doi: 10.1063/1.1143970
- Iyer S, Gaikwad RM, Subba-Rao V, Woodworth CD, Sokolov I (2009) Atomic force microscopy detects differences in the surface brush of normal and cancerous cells. *Nat Nanotechnol* 4:389-393. doi: 10.1038/nnano.2009.77
- Janmey PA, Euteneuer U, Traub P, Schliwa M (1991) Viscoelastic properties of vimentin compared with other filamentous biopolymer networks. *J Cell Biol* 113:155-160.
- Jazayeri R, Kwon YW (2011) Evolution of the reverse total shoulder prosthesis. *Bull NYU Hosp Jt Dis* 69:50-55.

- Karsai A, Martonfalvi Z, Nagy A, Grama L, Penke B, Kellermayer MS (2006) Mechanical manipulation of Alzheimer's amyloid beta1-42 fibrils. *J Struct Biol* 155:316-326. doi: 10.1016/j.jsb.2005.12.015
- Kellermayer MS (2011) Combined atomic force microscopy and fluorescence microscopy. *Methods Mol Biol* 736:439-456. doi: 10.1007/978-1-61779-105-5_27
- Kim KS, Cho CH, Park EK, Jung MH, Yoon KS, Park HK (2012) AFM-detected apoptotic changes in morphology and biophysical property caused by paclitaxel in Ishikawa and HeLa cells. *PLoS One* 7:e30066. doi: 10.1371/journal.pone.0030066
- Kumar S, LeDuc PR (2009) Dissecting the Molecular Basis of the Mechanics of Living Cells. *Experimental Mechanics* 49:11-23. doi: 10.1007/s11340-007-9063-7
- Kumar S, Weaver VM (2009) Mechanics, malignancy, and metastasis: The force journey of a tumor cell . *Cancer and Metastasis Reviews* 20:113-127. doi: 10.1007/s10555-008-9173-4
- Lee SY, Zaske AM, Novellino T, Danila D, Ferrari M, Conyers J, Decuzzi P (2011) Probing the mechanical properties of TNF-alpha stimulated endothelial cell with atomic force microscopy. *Int J Nanomedicine* 6:179-195. doi: 10.2147/IJN.S12760
- Levayer R, Lecuit T (2012) Biomechanical regulation of contractility: spatial control and dynamics. *Trends Cell Biol* 22:61-81. doi: 10.1016/j.tcb.2011.10.001
- Li QS, Lee GY, Ong CN, Lim CT (2008) AFM indentation study of breast cancer cells. *Biochem Biophys Res Commun* 374:609-613. doi: 10.1016/j.bbrc.2008.07.078
- Lichtman M, Gregory A, Kearney E (1973) Rheology of Leukocytes, Leukocyte Suspensions and Blood in Leukemia. *J Clin Invest* 52:350-358. doi: 10.1172/JCI107191
- Lieber SC, Aubry N, Pain J, Diaz G, Kim SJ, Vatner SF (2004) Aging increases stiffness of cardiac myocytes measured by atomic force microscopy nanoindentation. *Am J Physiol Heart Circ Physiol* 287:H645-51. doi: 10.1152/ajpheart.00564.2003
- Liu Y, Pinzon-Arango PA, Gallardo-Moreno AM, Camesano TA (2010) Direct adhesion force measurements between *E. coli* and human uroepithelial cells in cranberry juice

cocktail. *Mol Nutr Food Res* 54:1744-1752. doi: 10.1002/mnfr.200900535;
10.1002/mnfr.200900535

Lu L, Oswald SJ, Ngu H, Yin FC (2008) Mechanical Properties of Actin Stress Fibers in Living Cells. *Biophysical Journal* 95:6060-6071. doi: 10.1529/biophysj.108.133462

Mathur AB, Collinsworth AM, Reichert WM, Kraus WE, Truskey GA (2001) Endothelial, cardiac muscle and skeletal muscle exhibit different viscous and elastic properties as determined by atomic force microscopy. *Journal of Biomechanics* 34:1545-1553.

McGettrick HM, Hunter K, Moss PA, Buckley CD, Rainger GE, Nash GB (2009) Direct observations of the kinetics of migrating T cells suggest active retention by endothelial cells with continual bidirectional migration *Journal of Leukocyte Biology* 85:98-107.

McNamee CE, Pyo N, Higashitani K (2006) Atomic force microscopy study of the specific adhesion between a colloid particle and a living melanoma cell: Effect of the charge and the hydrophobicity of the particle surface. *Biophysical Journal* 91:1960-1969. doi: 10.1529/biophysj.106.082420

McNamee CE, Aso Y, Yamamoto S, Fukumori Y, Ichikawa H, Higashitani K (2007) Chemical groups that adhere to the surfaces of living malignant cells. *Pharm Res* 24:2370-2380. doi: 10.1007/s11095-007-9436-8

McNamee CE, Pyo N, Tanaka S, Vakarelski IU, Kanda Y, Higashitani K (2006) Parameters affecting the adhesion strength between a living cell and a colloid probe when measured by the atomic force microscope. *Colloids Surf B Biointerfaces* 48:176-182. doi: 10.1016/j.colsurfb.2006.01.014

Moreno-Flores S, Benitez R, Vivanco M, Toca-Herrera JL (2010a) Stress relaxation and creep on living cells with the atomic force microscope: a means to calculate elastic moduli and viscosities of cell components. *Nanotechnology* 21:445101. doi: 10.1088/0957-4484/21/44/445101

Moreno-Flores S, Benitez R, Vivanco MD, Toca-Herrera JL (2010b) Stress relaxation microscopy: imaging local stress in cells. *J Biomech* 43:349-354. doi: 10.1016/j.jbiomech.2009.07.037

Muller WA (2011) Mechanisms of leukocyte transendothelial migration. *Annu Rev Pathol* 6:323-344. doi: 10.1146/annurev-pathol-011110-130224

Oberleithner H, Callies C, Kusche-Vihrog K, Schillers H, Shahin V, Riethmuller C, Macgregor GA, de Wardener HE (2009) Potassium softens vascular endothelium and increases nitric oxide release. *Proc Natl Acad Sci U S A* 106:2829-2834. doi: 10.1073/pnas.0813069106

Oberleithner H, Riethmuller C, Schillers H, MacGregor GA, de Wardener HE, Hausberg M (2007) Plasma sodium stiffens vascular endothelium and reduces nitric oxide release. *Proceeding of the National Academy of Sciences* 104:16281-16286. doi: 10.1073/pnas.0707791104

O'Callaghan R, Job KM, Dull RO, Hlady V (2011) Stiffness and heterogeneity of the pulmonary endothelial glycocalyx measured by atomic force microscopy. *Am J Physiol Lung Cell Mol Physiol* 301:L353-60. doi: 10.1152/ajplung.00342.2010

Panorchan P, Thompson MS, Davis KJ, Tseng Y, Konstantopoulos K, Wirtz D (2006) Single-molecule analysis of cadherin-mediated cell-cell adhesion. *Journal of Cell Science* 119:66-74. doi: 10.1242/jcs.02719

Pelling AE, Veraitch FS, Chu CP, Mason C, Horton MA (2009) Mechanical dynamics of single cells during early apoptosis. *Cell Motil Cytoskeleton* 66:409-422. doi: 10.1002/cm.20391

Perrault CM, Bray EJ, Didier N, Ozaki CK, Tran-Son-Tay R (2004) Altered rheology of lymphocytes in the diabetic mouse. *Diabetologia* 47:1722-1726. doi: 10.1007/s00125-004-1524-2

Picco LM, Bozec L, Ulcinas A, Engledew DJ, Antognozzi M, Horton MA, Miles MJ (2007) Breaking the speed limit with atomic force microscopy. *Nanotech* 18:doi: 10.1088/0957-4484/18/4/044030

Pogoda K, Jaczewska J, Wiltowska-Zuber J, Klymenko O, Zuber K, Fornal M, Lekka M (2012) Depth-sensing analysis of cytoskeleton organization based on AFM data. *Eur Biophys J* 41:79-87. doi: 10.1007/s00249-011-0761-9

- Robert P, Sengupta K, Puech PH, Bongrand P, Limozin L (2008) Tuning the formation and rupture of single ligand-receptor bonds by hyaluronan-induced repulsion. *Biophys J* 95:3999-4012. doi: 10.1529/biophysj.108.135947
- Rosenberg GA (2012) Neurological diseases in relation to the blood-brain barrier. *J Cereb Blood Flow Metab* 32:1139-1151. doi: 10.1038/jcbfm.2011.197; 10.1038/jcbfm.2011.197
- Rosenbluth MJ, Crow A, Shaevitz JW, Fletcher DA (2008) Slow stress propagation in adherent cells. *Biophys J* 95:6052-6059. doi: 10.1529/biophysj.108.139139
- Rosenbluth MJ, Lam WA, Fletcher DA (2006) Force microscopy of nonadherent cells: a comparison of leukemia cell deformability. *Biophys J* 90:2994-3003. doi: 10.1529/biophysj.105.067496
- Schillers H, Walte M, Urbanova K, Oberleithner H (2010) Real-time monitoring of cell elasticity reveals oscillating myosin activity. *Biophys J* 99:3639-3646. doi: 10.1016/j.bpj.2010.09.048
- Shelby JP, White J, Ganesan K, Rathod PK, Chiu DT (2003) A microfluidic model for single-cell capillary obstruction by *Plasmodium falciparum*-infected erythrocytes. *Proc Natl Acad Sci U S A* 100:14618-14622. doi: 10.1073/pnas.2433968100
- Sheng X, Ting YP, Pehkonen SO (2007) Force measurements of bacterial adhesion on metals using a cell probe atomic force microscope. *J Colloid Interface Sci* 310:661-669. doi: 10.1016/j.jcis.2007.01.084
- Sneddon IN (1965) The relation between load and penetration in the axisymmetric boussinesq problem for a punch of arbitrary profile. *International Journal of Engineering Science* 3:47-57.
- Stroka KM, Aranda-Espinoza H (2011) Effects of Morphology vs. Cell-Cell Interactions on Endothelial Cell Stiffness. *Cell Mol Bioeng* 4:9-27. doi: 10.1007/s12195-010-0142-y
- Sunyer R, Trepas X, Fredberg JJ, Farre R, Navajas D (2009) The temperature dependence of cell mechanics measured by atomic force microscopy. *Phys Biol* 6:025009. doi: 10.1088/1478-3975/6/2/025009

Suresh S (2007) Biomechanics and biophysics of cancer cells. *Acta Biomater* 3:413-438. doi: 10.1016/j.actbio.2007.04.002

Tan JL, Tien J, Pirone DM, Gray DS, Bhadriraju K, Chen CS (2003) Cells lying on a bed of microneedles: an approach to isolate mechanical force. *Proc Natl Acad Sci U S A* 100:1484-1489. doi: 10.1073/pnas.0235407100

Trepat X, Fredberg JJ (2011) Plithotaxis and emergent dynamics in collective cellular migration. *Trends Cell Biol* 21:638-646. doi: 10.1016/j.tcb.2011.06.006

Ubbink J, Schar-Zammaretti P (2005) Probing bacterial interactions: integrated approaches combining atomic force microscopy, electron microscopy and biophysical techniques. *Micron* 36:293-320. doi: 10.1016/j.micron.2004.11.005

van der Meer AD, Vermeul K, Poot AA, Feijen J, Vermes I (2010) A microfluidic wound-healing assay for quantifying endothelial cell migration. *Am J Physiol Heart Circ Physiol* 298:H719-25. doi: 10.1152/ajpheart.00933.2009

van Mameren J, Wuite GJ, Heller I (2011) Introduction to optical tweezers: background, system designs, and commercial solutions. *Methods Mol Biol* 783:1-20. doi: 10.1007/978-1-61779-282-3_1

Végh AG, Nagy K, Bálint Z, Kerényi A, Rákhely G, Váró G, Szegletes Z (2011) Effect of antimicrobial Peptide-amide: indolicidin on biological membranes. *J Biomed Biotechnol* 2011:670589. doi: 10.1155/2011/670589

Vinckier A, Semenza G (1998) Measuring elasticity of biological materials by atomic force microscopy. *FEBS Letters* 430:12-16.

Wagh AA, Roan E, Chapman KE, Desai LP, Rendon DA, Eckstein EC, Waters CM (2008) Localized elasticity measured in epithelial cells migrating at a wound edge using atomic force microscopy. *Am J Physiol Lung Cell Mol Physiol* 295:L54-60. doi: 10.1152/ajplung.00475.2007

Wang N, Butler JP, Ingber DE (1993) Mechanotransduction across the cell surface and through the cytoskeleton. *Science* 260:1124-1127.

Wilhelm I, Fazakas C, Krizbai IA (2011) In vitro models of the blood-brain barrier. *Acta Neurobiol Exp (Wars)* 71:113-128.

Wilhelm I, Nagyoszi P, Farkas AE, Couraud PO, Romero IA, Weksler B, Fazakas C, Dung NT, Bottka S, Bauer H, Bauer HC, Krizbai IA (2008) Hyperosmotic stress induces Axl activation and cleavage in cerebral endothelial cells. *J Neurochem* 107:116-126. doi: 10.1111/j.1471-4159.2008.05590.x

Wilhelm I, Farkas EA, Nagyoszi P, Váró G, Végh AG, Couraud P, Bálint Z, Weksler B, Krizbai IA, Romero AI (2007) Regulation of cerebral endothelial cell morphology by extracellular calcium. *Physics in Medicine and Biology* 52:6261-6274.

Wojcikiewicz EP, Abdulreda MH, Zhang X, Moy VT (2006) Force spectroscopy of LFA-1 and its ligands, ICAM-1 and ICAM-2. *Biomacromolecules* 7:3188-3195. doi: 10.1021/bm060559c

Wu HW, Kuhn T, Moy VT (1998) Mechanical properties of L929 cells measured by atomic force microscopy: effects of anticytoskeletal drugs and membrane crosslinking. *Scanning* 20:389-397.

Wu Y, Yu T, Gilbertson TA, Zhou A, Xu H, Nguyen KT (2012) Biophysical assessment of single cell cytotoxicity: diesel exhaust particle-treated human aortic endothelial cells. *PLoS One* 7:e36885. doi: 10.1371/journal.pone.0036885

Yang R, Chen JY, Xi N, Lai KW, Qu C, Fung CK, Penn LS, Xi J (2012) Characterization of mechanical behavior of an epithelial monolayer in response to epidermal growth factor stimulation. *Exp Cell Res* 318:521-526. doi: 10.1016/j.yexcr.2011.12.003

Yuan C, Chen A, Kolb P, Moy VT (2000) Energy landscape of streptavidin-biotin complexes measured by atomic force microscopy. *Biochemistry* 39:10219-10223.

Zhang T, Chao Y, Shih K, Li XY, Fang HH (2011) Quantification of the lateral detachment force for bacterial cells using atomic force microscope and centrifugation. *Ultramicroscopy* 111:131-139. doi: 10.1016/j.ultramic.2010.10.005

Zhang X, Chen A, De Leon D, Li H, Noiri E, Moy VT, Goligorsky MS (2003) Atomic force microscopy measurement of leukocyte-endothelial interaction. *American Journal of*

Physiology - Heart and Circular Physiology 286:H359-H367. doi:
10.1152/ajpheart.00491.2003

Zhang X, Wojcikiewicz EP, Moy VT (2006) Dynamic Adhesion of T Lymphocytes to Endothelial Cells Revealed by Atomic Force Microscopy. *Experimental Biology and Medicine* 231:1306-1312.

Zhang Y, Sivasankar S, Nelson JW, Chu S (2009) Resolving cadherin interactions and binding cooperativity at the single-molecule level. *Proceeding of the National Academy of Sciences* 106:109-114. doi: 10.1073/pnas.0811350106

Aknowledgement

This thesis is the fruit of work of my studies in the Institute of Biophysics, Biological Research Centre of the Hungarian Academy of Sciences. I have got support, guidance and advices from many people to whom I am truly grateful.

First, I would like to express my deepest gratitude to my supervisor, Dr. György Váró, who introduced me to the field of biophysics. I was impressed and inspired by his way of thinking about science and life. His careful guidance developed my experimental skills and our everyday debates about the projects broadened my knowledge and made my work and life easier. I would like to thank Dr. Pál Ormos, the director of the Institute of Biophysics, and all members of the Institute for creating a stimulating atmosphere and giving interesting feedbacks and valuable discussions.

I wish to acknowledge my colleagues, Dr. Zoltán Bálint, Dr. Zsolt Szegletes and Krisztina Nagy for invaluable discussions we had and useful advices they gave me during my work. I am grateful to Dr. Imola Wilhelm and Dr. István A. Krizbai for the cell cultures, cell biology background and invaluable discussions.

Particular appreciation regards the German representatives of the Asylum Research Company, especially Stefan Vinzelberg, Friedhelm Freiss and many others for the continuous assistance and technical help.

I have to express my grateful appreciation to my wife Csilla Fazakas. Her daily scientific and social support was absolutely necessary to fulfill this task. Special gratitude to all my family and friends, teachers and colleagues, for support and keeping me on the path during all my education, especially for my PhD thesis, with “show must go on”- like conversations and guidance.

This work was supported by the following grants: OTKA-K 81180, OTKA-K 100807.

Annex